Journal of Energy Storage 166 (2026) 122318

Contents lists available at ScienceDirect

Journal of Energy Storage

journal homepage: www.elsevier.com/locate/est

Research Papers

Experimental and numerical investigation on the performance and cost analysis of an innovative thermal storage wall

Cansu Bekler [a,c], İdil Ayçam [a], Mustafa Zeki Yılmazoğlu [b,*], Asena Soyluk [a]

[a] Department of Architecture, Faculty of Architecture, Gazi University, Ankara, Türkiye
[b] Department of Mechanical Engineering, Faculty of Engineering, Gazi University, Ankara, Türkiye
[c] Nevşehir Hacı Bektaş Veli University, Faculty of Engineering and Architecture, Department of Architecture, Nevşehir, Türkiye

ARTICLE INFO

Keywords:
Transparent insulation
Phase change material
Energy storage
Thermal comfort
Energy efficiency

ABSTRACT

Innovative building envelopes made from advanced materials play a critical role in improving energy performance by enhancing the effective thermal mass of buildings within passive design strategies. This study proposes a passive wall system integrating transparent insulation material (TIM) with a PCM-embedded brick wall (TIM-AG-PCM wall) to improve building thermal performance during both heating and cooling seasons. The innovative wall system was initially configured through mathematical analysis, and its alternative wall system configurations were experimentally compared under the continental climatic conditions of Ankara using instantaneous measurement data to determine the highest-performing configuration. The selected system was subsequently integrated at the building scale and modeled parametrically for each facade with application ratios ranging from 20% to 100%. For each ratio, energy performance and cost data were obtained and normalized to determine the optimum application ratios. The results indicate that applying the TIM-AG-PCM wall at ratios of 35–40% on the south facade, 50% on the north facade, and 50–60% on the east and west facades provides an optimal balance between thermal performance and cost, offering a sustainable and efficient design solution for building envelopes. At these optimum ratios, building energy consumption was reduced by 25.8% compared to a conventional wall system. Annual analyses further reveal that the hybrid use of two PCMs with different melting temperatures, selected for heating and cooling seasons, supports continuous thermal regulation during transitional periods.

Nomenclature

U	Thermal transmittance [W/m^2 K]
X	Thickness [cm]
C_p	Specific heat capacity [J/kg·K]
TIM	Transparent insulation material
PCM	Phase change material
AG	Air gap
COP	Coefficient of performance
PP	Payback period
C_y($)	Annual energy cost [$]
C_h	Annual heating energy cost [$]
C_c	Annual cooling energy cost [$]
C_f	The unit price of the fuel [$/m^3]
$C_{TIM-AG-PCM\ WALL}$	The cost of the TIM-AG-PCM wall [$/m^2]
H_u	The lower heating value of the fuel (kWh/m^3)
C_e	The unit price of electricity ($/kWh)
C_T	The cost of the TIM-AG-PCM wall [$/m^2]
C_{yyt}	The annual fuel saving [$/m^2]
C_{dek}	The annual energy cost of the dwelling with the transparent insulation latent heat storage wall [$/m^2]

Greek letters

λ	Thermal conductivity [W/m·K]
ρ	Density [kg/m^3]
α_G	Absorptivity
ρ_{solid}	The density of a material in its solid phase [kg/m^3]
ρ_{liquid}	The density of a material in its liquid phase [kg/m^3]

* Corresponding author.
E-mail address: zekiyilmazoglu@gazi.edu.tr (M.Z. Yılmazoğlu).

https://doi.org/10.1016/j.est.2026.122318
Received 13 November 2025; Received in revised form 23 March 2026; Accepted 19 April 2026
Available online 27 April 2026
2352-152X/© 2026 Published by Elsevier Ltd.

1. Introduction

Energy is regarded as the backbone of human activity, and the global population that drives energy demand continues to rise [1]. Proportionally to this increase, the construction sector—which accounts for a substantial share of global energy consumption, primarily due to heating and cooling demands—has expanded rapidly [2]. As global energy demand and, consequently, greenhouse gas emissions continue to rise, researchers have been seeking greener alternatives for energy storage and supply.

To reduce energy consumption in buildings and to enable low-energy building applications, various passive solar technologies are implemented within the building envelope. The optical and thermophysical properties of the materials used in the multilayer structure of walls in such systems play a crucial role in determining the amount of heat gained or lost per unit area of the wall under the combined effects of outdoor temperature and solar radiation. Another important parameter to be considered in passive heat-storage wall designs is the prevention of heat loss through the wall surfaces. Opaque insulation materials applied to the inner or outer surface of a wall can effectively prevent heat loss from the indoor to the outdoor environment during winter. However, such opaque materials cannot take advantage of solar gains through passive means during the heating season.

Transparent insulation materials (TIMs), on the other hand, differ from conventional insulation materials due to their solar transmittance property. When used as insulation in transparent or semi-transparent wall assemblies, TIMs not only high thermal insulation but also contribute to daylighting in interior spaces. When applied in front of opaque walls, they enhance the thermal mass performance of the wall by combining their high insulation capacity with radiative heat transfer effects.

Another passive design approach for reducing building energy demand involves the use of thermal mass for energy storage. During sunny winter days, solar radiation absorbed by the wall is stored in the thermal mass, and at night—when solar radiation is absent—the stored energy is released into the indoor environment with a time delay, depending on the material's properties. In this way, indoor comfort conditions are passively maintained, and the building's heating energy demand is reduced. Recently, the use of phase change materials (PCM), which store heat in the form of latent heat rather than sensible heat, has emerged as a promising method for enhancing building thermal performance. PCMs absorb a significant amount of heat energy while maintaining nearly constant temperature during phase transitions (solid–liquid or liquid–gas), and they release stored heat when reverting to a lower phase (liquid–solid or gas–liquid). Consequently, PCM improve thermal comfort while reducing overall energy demand and peak heating-cooling loads [3–6].

For PCMs integrated into the building envelope to achieve the desired performance, the melting/solidification temperature must be selected according to the climatic conditions of the application region, the position of the multilayer building components must consider the thermophysical properties of all layers, and the integration method must ensure proper structural and thermal coupling.

The first studies on TIM and PCM-integrated wall systems were conducted at the Laboratory for Heating, Sanitary, and Solar Technology of the Faculty of Mechanical Engineering in Ljubljana [7]. In that research, the wall layers were defined, from outside to inside, as a glass panel protecting the TIM from outdoor conditions, followed by the TIM itself, PCM placed within a transparent plastic frame, an air gap, insulation, and plaster. Manz et al. [8] proposed a semi-transparent TIM-PCM wall in which PCM-integrated glass bricks were connected to the TIM insulation unit through an air cavity. To prevent overheating caused by the high solar transmittance of TIM, a shading device (roller blind) was incorporated. Kienzl [9] further developed this concept by placing an electrochromic glass in front of the TIM, enabling controlled solar gain and enhancing PCM effectiveness. Heim [10,11] focused on the application of transparent insulation in front of walls by impregnating PCM into the wall material, transforming it into a high-energy-storage structural element connected to a transparent insulation unit via an air gap. Subsequent studies have proposed various innovations to improve the performance of semi-transparent TIM-PCM walls under both summer and winter conditions [12–14].

Research supported by numerical, simulation, and experimental methods has shown that TIM-PCM walls effectively stabilize indoor comfort conditions, improve building performance, and reduce energy consumption. Most studies on TIM-PCM walls, however, have focused on semi-transparent wall types. In opaque wall applications, direct inclusion and impregnation techniques are generally used to integrate PCMs into materials. The main challenge with these methods lies in potential leakage problems and adverse effects on the mechanical properties and durability of the structure. In contrast, embedding encapsulated PCM within wall materials avoids such issues and offers greater on-site applicability. For this reason, studies involving TIM-PCM walls with PCM embedded into the wall material were examined, revealing a gap in this specific research area.

This study addresses that gap by presenting a comprehensive performance analysis of an opaque TIM-AG-PCM wall composed of a transparent insulation unit filled with aerogel granules between two glass panes, combined with a composite brick body containing encapsulated PCM, and separated by a ventilated air gap. The analysis was conducted through three sequential methodological stages, and the results were discussed under the themes of design, performance, and cost to provide an integrated evaluation of the innovative wall system. In previous studies, wall systems were evaluated solely from a performance perspective; building-scale analyses were not conducted, and design considerations were overlooked. Filling this gap highlights the originality and holistic approach of the present study. The proposed TIM-AG-PCM wall differs from previous designs with its unique configuration. The design decision to incorporate two types of PCMs—each optimized for different thermal seasons—equally within the wall structure allows the wall to perform effectively during heating, cooling, and intermediate seasons, thereby offering a comprehensive solution to the dual-season performance challenge.

2. Material and methods

An evaluation strategy consisting of five interrelated methodological steps was established to verify the hypothesis proposed within the scope of the study (Fig. 1).

Within the methodological framework, a literature review was conducted to determine the climatic region in which the analyses would be performed as well as the indoor boundary conditions. Based on this review, the materials to be used in the TIM-AG-PCM wall system, their positions within the wall layers, and their respective thicknesses were defined. In the subsequent step, the explicit finite difference method was employed in the MATLAB code developed for the study to numerically solve the one-dimensional transient heat transfer equation. For the TIM-AG-PCM wall system, temperature values were obtained at spatial intervals of 0.004 m with a time step of 1.2 s [15]. Based on the mathematical analysis, the PCM type that performs effectively under the climatic conditions of the analyzed region was identified, and the performance of the innovative wall was revealed by comparing its temperature data with that of a standard wall analyzed under identical boundary and environmental conditions.

The studies conducted up to the third methodological step of the evaluation strategy encompass the assessment of analyses performed through mathematical functions derived from defined boundary conditions and the annual average climatic values of the region, based on the wall cross-section. In this investigation, further analyses focus on determining the actual performance of the TIM-AG-PCM wall under real conditions at the building scale, examining how its performance varies with orientation and the proportion of use on each facade, and

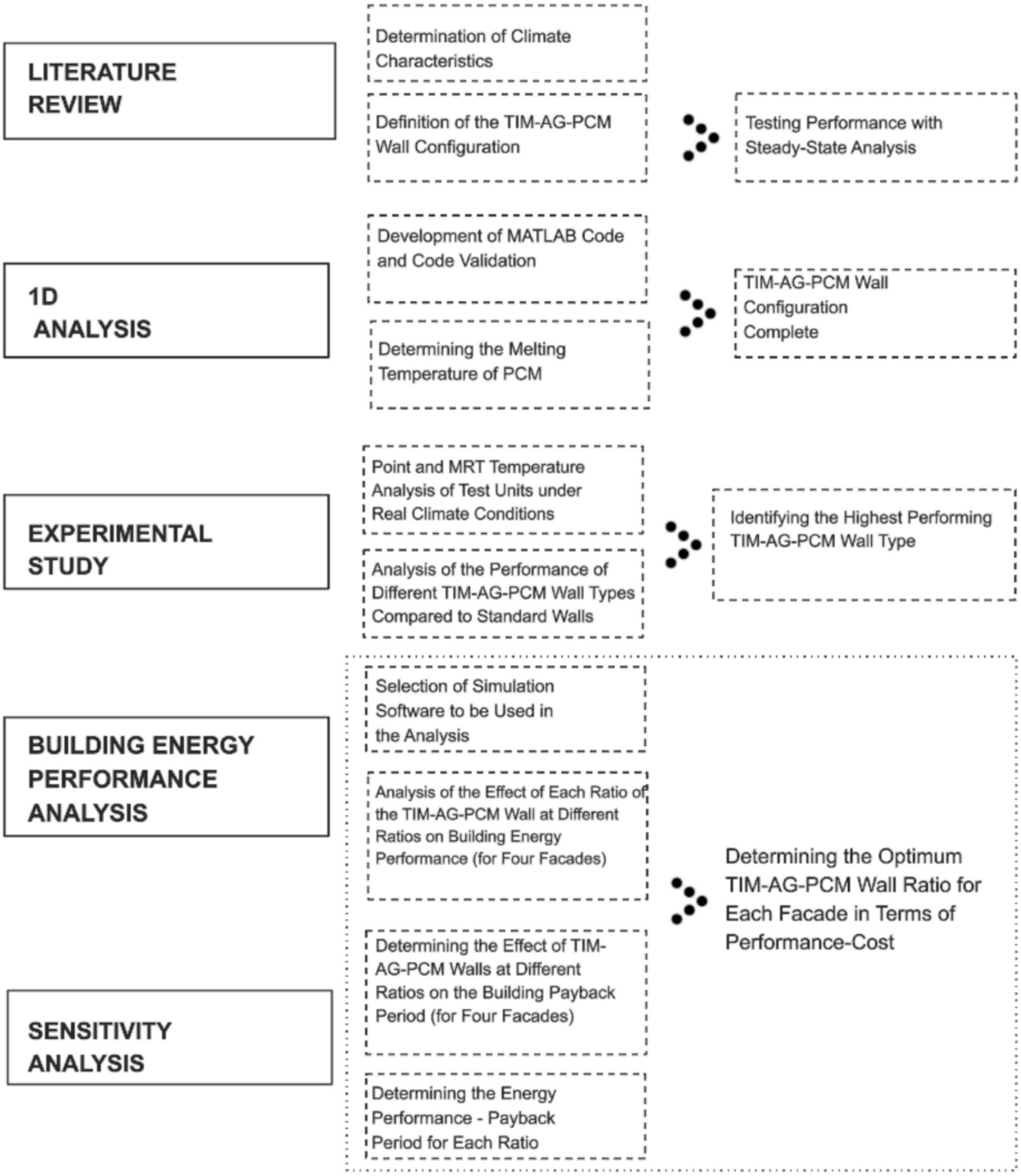


Fig. 1. Evaluation strategy of the study.

evaluating the obtained performance data in the context of cost to determine the optimal TIM-AG-PCM ratio for each facade.

2.1. *Experimental study*

The configuration of the transparent insulation and latent heat storage wall, which is based on determining the layer thicknesses of the materials used and their positions within the wall section, as well as the performance analysis of the wall under the climatic conditions of Ankara, was revealed through a time-dependent mathematical analysis [15]. As a result of this study, it was determined that among the components of the TIM-AG-PCM wall, the PCM type RT18HC performs effectively during the heating season and RT22HC during the cooling season for the climatic region where the measurements were taken. Based on this result, a design decision demonstrating the originality of the TIM-AG-PCM wall was established (Fig. 2).

Experimental studies were conducted in a designated area on the campus of Gazi University Faculty of Architecture in Ankara, Türkiye, to analyze the real-scale performance of the TIM-AG-PCM wall under actual environmental conditions (Fig. 3).

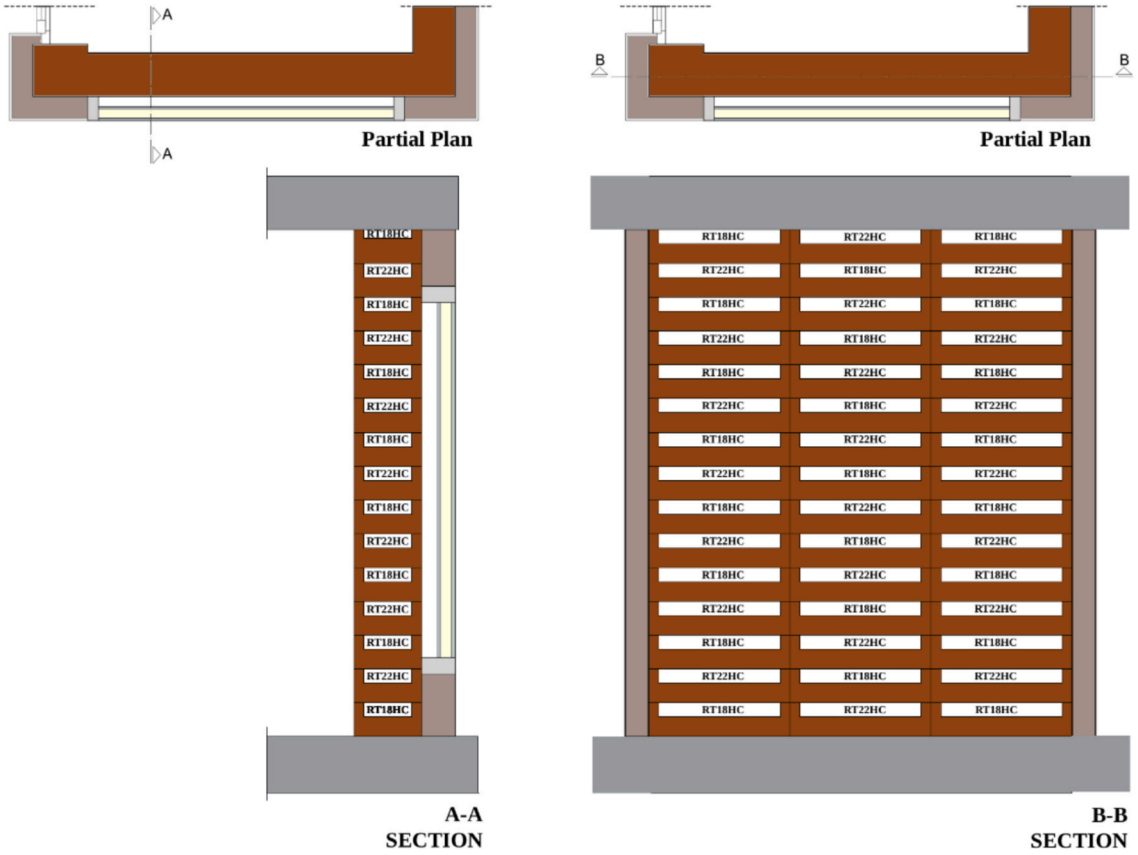


Fig. 2. Cross-section of the TIM-AG-PCM wall and the brick arrangement integrating PCMs with different melting temperatures.



Fig. 3. Satellite view of the area where the experimental chambers were constructed (Google Earth).

Four experimental chambers, each with a volume of 1 m^3, were constructed in the designated area. Three of these experimental chambers had different types of TIM-AG-PCM wall configurations integrated into their south facades. To compare the obtained results, an additional reference chamber was constructed with standard wall configurations on all four facades, as generally used in the Turkish construction sector, and simultaneous measurements were taken from all four experimental chambers (Fig. 4).

The experimental chambers with different TIM-AG-PCM wall configurations on their south facades (Chamber 1, Chamber 2, and Chamber 3) had standard wall configurations on the remaining three facades. In Chamber 1, a 2 cm air gap was provided between the TIM unit and the PCM-integrated wall. In Chamber 2, a 5 cm air gap was placed between the TIM unit and the PCM-integrated wall. In this TIM-AG-PCM wall type, 8 cm × 50 cm vents were positioned at the top and bottom parts of the PCM-integrated wall. The surfaces of these vents facing the chamber were equipped with small covers that could be opened and closed during daytime and nighttime in both heating and cooling seasons. In Chamber 3, a 10 cm unventilated gap was left between the TIM unit and the PCM-integrated wall, and a white roller blind, which could be manually operated during daytime and nighttime in both heating and cooling seasons, was placed inside the gap. Chamber 4 consisted of standard walls on all four facades (Fig. 4). All experimental chambers had a 75 cm × 75 cm openable sash window on the east facade. The thickness of the insulation (XPS) used in the standard wall configuration of the test chambers was determined in accordance with TS 825 (2008). The thermophysical properties of the materials used in the wall elements of the experimental chambers are given in Table 1.

In the TIM-AG-PCM integrated configurations of the test chambers, temperature measurements were obtained using K-type thermocouples at the locations indicated in the cross-section shown in Table 2. The measurement points included: the outermost glass surface exposed to the exterior environment (a); the inner surface of the glass facing the air gap (b); the surfaces of the RT18HC- and RT22HC-integrated bricks facing the air gap (c); the interface surfaces between the RT18HC and RT22HC materials and the adjacent brick elements (d); the interior-facing surfaces of the RT18HC- and RT22HC-integrated bricks (e); and the center of the indoor air volume within the test chamber (f). Instantaneous temperature data collected from a total of 30 measurement

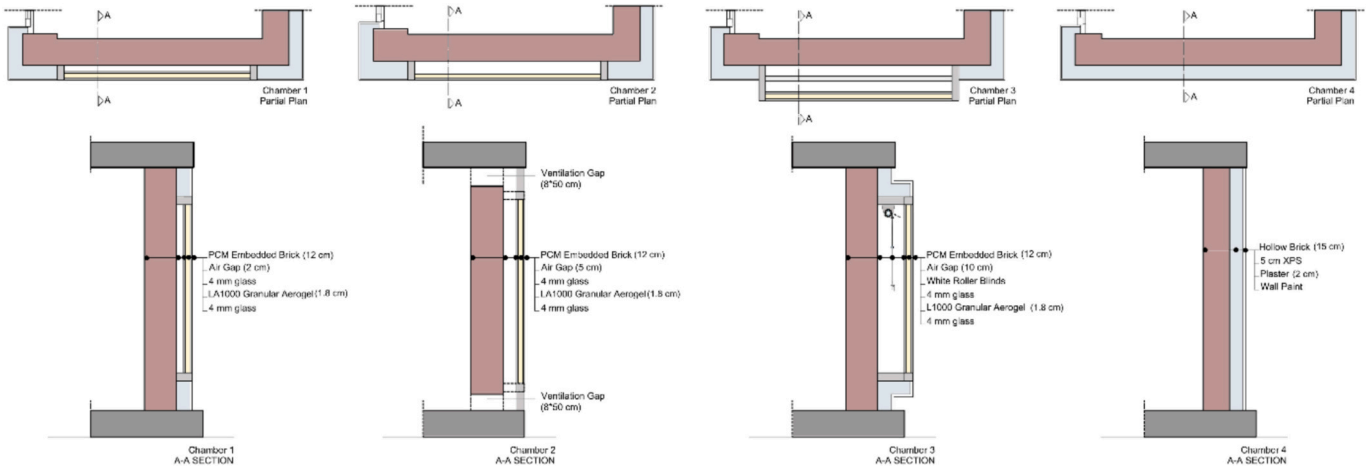


Fig. 4. Experimental chambers constructed for the experimental study.

Table 1
Thermophysical properties of materials used in the wall elements of experimental chambers.

	X (cm)	λ [W/m K]	C_P [J/kg K]	ρ_{solid} [kg/m^3]	ρ_{liquid} [kg/m^3]
Glass	0.4	0.95	800	2225	–
Plaster	2	0.3	1050	1800	
Granular aerogel	1.6	0.012	1150	120	–
Clay brick	12	0.32	840	600	–
Hollow brick	15	0,40	840	1920	
XPS	5	0.034	1380	24	–
RT18HC	8.5	0.2	2000	880	770
RT22HC	8.5	0.2	2000	760	700

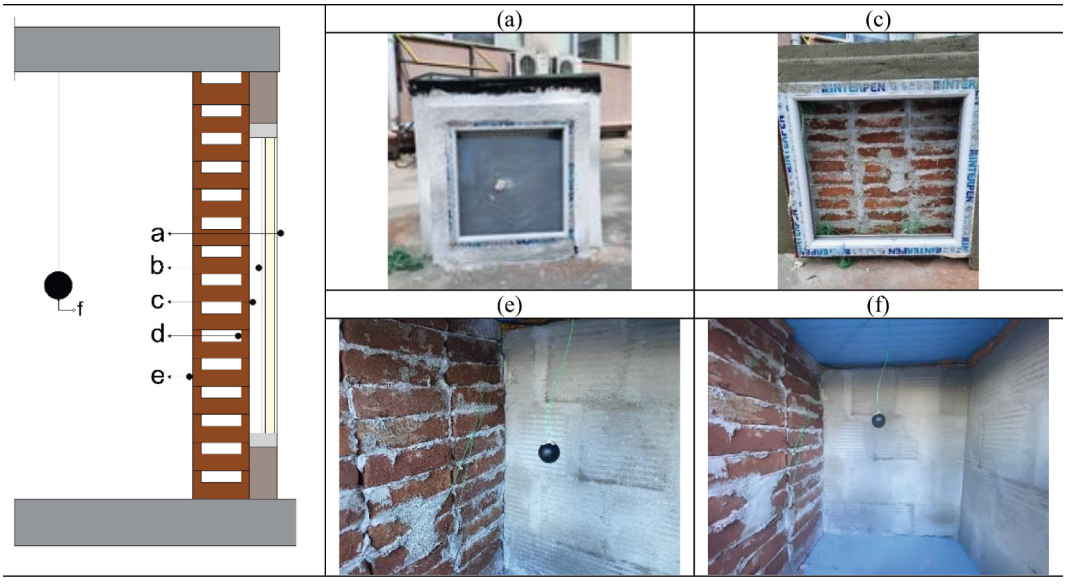
points were recorded using a 45-channel HIOKI LR8450 data logger. In addition to the instantaneous temperature measurements obtained from the experimental chambers, real-time solar radiation intensity data were also recorded using an EKO MS-802 pyranometer, which was connected to the datalogger to monitor the influence of solar radiation.

2.2. Simulation

The simulation tool used to evaluate the impact of the highest-performing TIM-AG-PCM wall, identified through experimental measurements, on building energy performance was selected based on a review of previous studies. The simulation tool used to analyze the impact of the highest-performing TIM-AG-PCM wall, which was determined through experimental measurements on building energy performance, was selected based on the analysis of previous studies. A review of energy simulation tools and their usage frequencies revealed that EnergyPlus is the most widely used energy simulation program for PCM-integrated building and aerogel glazing system simulations [16–23]. The second most frequently used software is DesignBuilder [24], which is also based on the EnergyPlus simulation engine [25–32].

DesignBuilder is a software tool developed to evaluate and control building performance in terms of energy, carbon, lighting, and comfort by using the EnergyPlus simulation engine (Altensis [33]). Owing to its user-friendly interface, the use of the EnergyPlus simulation engine, and its proven validity and reliability through its extensive use in numerous scientific studies, DesignBuilder was selected as the simulation tool for

Table 2
Locations where thermocouples are placed in the experimental chambers.



this study.

The reference residential building to be modeled for the simulation was selected from the TOKI Turkuaz Valley Housing Project in Ankara, Türkiye, since TOKI constructs residential buildings across all provinces in the country. The CK-type floor plan of the 2 + 1 apartment, with a gross area of 85 m^2, was used (Fig. 5). The apartment consists of a living room, an open kitchen, and two bedrooms. On the south facade are the living room, kitchen, and bedroom; on the east facade, the master and children's bedrooms; on the north facade, the master bedroom, bathroom, and toilet; and on the west facade, the entrance and kitchen. The reference building comprises 14 storeys with four identical apartments per floor; however, the multi-storey structure was not considered in the simulation. For the purposes of this study, a representative apartment plan was selected and modeled as an independent single-storey unit. Accordingly, multi-storey building effects such as inter-zone airflows and complex thermal mass interactions were not included in the thermal analysis. This approach focuses on the impact of the TIM-AG-PCM wall system used in the building envelope of a single-storey unit on thermal performance.

The materials used in the building envelope components of the reference model were determined according to the material specifications used in TOKI construction projects. The materials and their corresponding thermal properties are presented in Table 3.

For the building energy simulation analyses, the 2023 climatic data for Ankara, Etimesgut, obtained from Meteonorm [34], were used. The assumptions and limitations defined for the analyses were as follows: to evaluate the impact on heating and cooling loads, it was assumed that during the cooling season, a split-type AC system was used, while during the heating season, a natural gas-based wall-hang boiler system was employed, and no mechanical ventilation was included. It was also assumed that a family of three occupied the apartment to account for internal heat gains. The indoor air temperature was set to 21 °C for the heating season and 24 °C for the cooling season. The TIM-AG-PCM Wall Type-3 was centered on the middle of the facade where it was applied to

Table 3
U-value of the building envelope components of the reference residential building.

Component	U [W/m^2K]
Roof	0.335
Wall	0.455
TIM-AG-PCM wall	0.155
Ground	0.202
Window	2.715
PVC frame	2.155

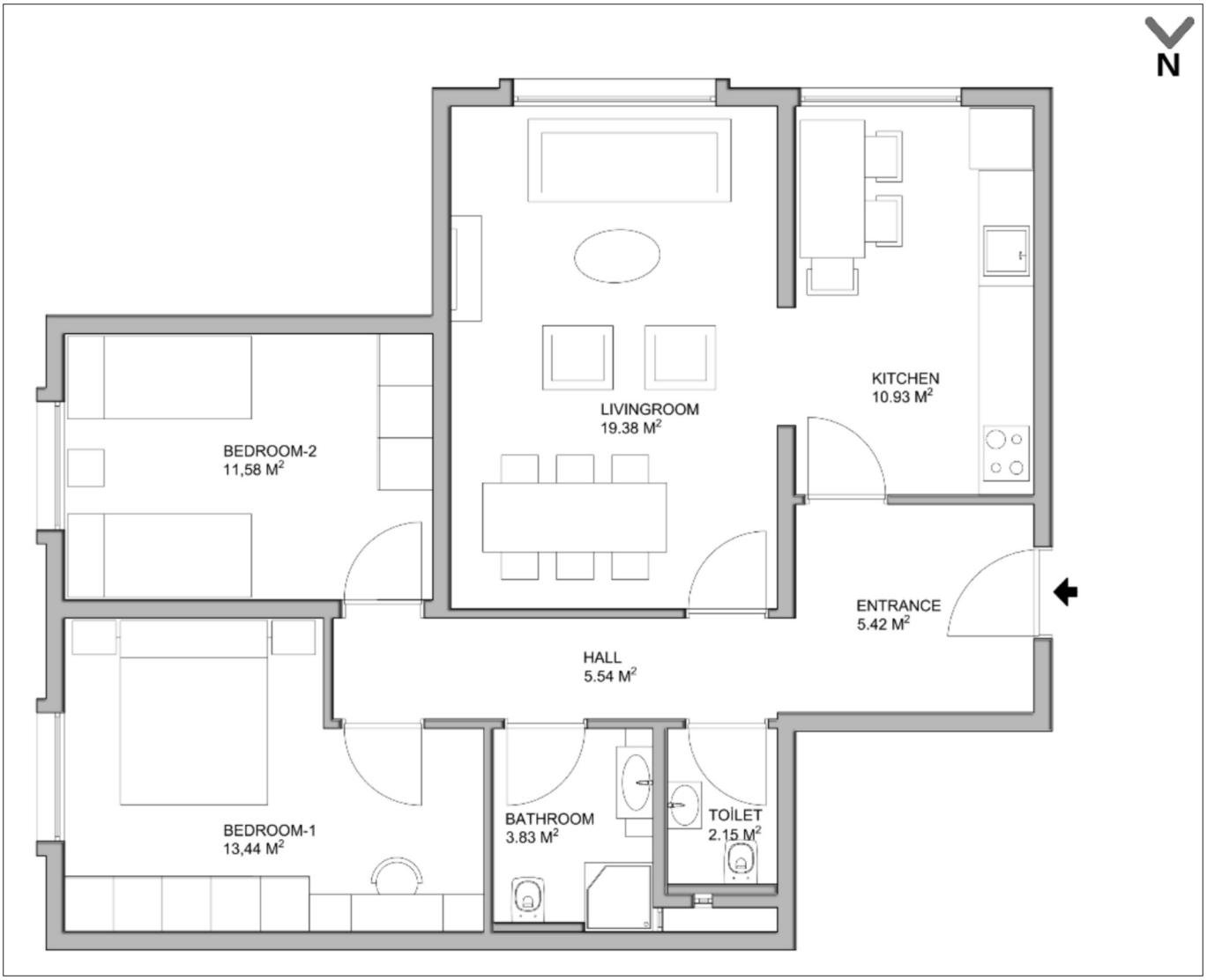


Fig. 5. A single-storey reference residential building plan to be tested using the simulation tool.

avoid corner effects on the mean radiant temperature.

To accurately analyze the influence of PCM on the energy load, it is essential to define the temperature range of the heating and cooling systems. Therefore, it was assumed that the apartment was heated between 17 °C and 21 °C during the heating season and cooled between 25 °C and 28 °C during the cooling season. For the space where the PCM-integrated wall was applied, the heating temperature range was adjusted to 17 °C–19 °C, and the cooling setpoint range to 22 °C–24 °C, to prevent the indoor air temperature from adversely affecting PCM operation.

To account for realistic internal heat gains, the equipment within the apartment was activated in accordance with the functional use of each space and operated according to a defined schedule to generate heat. This ensured that the calculated heating and cooling loads reflected realistic energy demand conditions. A simple HVAC system was selected for the analysis, allowing for the calculation of ideal loads.

2.3. Sensitivity analysis

This section aims to define the design variables required to achieve sensitivity analysis of the TIM-AG-PCM wall system in terms of dimensional efficiency and cost-effectiveness when integrated into the building envelope. Using the identified design variables, the performance of the reference residential building—where the wall system is applied to different architectural configurations—was evaluated through simulations conducted with the DesignBuilder code.

A literature review was conducted to determine suitable design variables, revealing that previous studies categorized the main design parameters under three primary headings: building envelope, mechanical systems, and building form, each comprising specific design sub-parameters [35–42,54]. Based on the evaluation of these sub-parameters, design variables relevant to the proposed wall system were selected to enable its performance assessment under various architectural configurations for optimum sizing and cost-efficiency.

The first design variable identified was the window-to-wall ratio (WWR). In this study, the window-to-wall ratio of the TOKI Turkuaz residential building's CK-type floor plan was preserved. The opaque wall area was considered as the applicable surface for the TIM-AG-PCM wall, and its ratio varied incrementally from 0% to 100% at 20% intervals. To determine the optimal proportion of the TIM-AG-PCM wall on each facade, simulations were conducted assuming that 20% of the selected facade was covered by the innovative wall, and then progressively increasing this proportion while keeping the other three facades in their original configuration. For each ratio, heating load, cooling load, and mean indoor temperature values were obtained. Thus, it has also contributed to the assessments made regarding the orientation parameter, which is another design variable.

Using these defined design variables, data were collected regarding the energy performance and cost-effectiveness of the TIM-AG-PCM wall system for different ratios on each facade. The relationship between these variables was established through min–max normalization, in which the lowest and highest values within the dataset were identified and all other data were normalized between 0 and 1 according to these extremes [43]. The purpose of this method is to place all data within a common numerical scale by assigning 0 to the minimum value and 1 to the maximum value, enabling direct comparison across datasets (Eq. (1)).

$$X_{normal} = \frac{X - X_{\min.}}{X_{mak.} - X_{\min.}} \tag{1}$$

In this approach, energy performance and payback period were considered as equally prioritized criteria, and the analysis was conducted under the assumption of a “neutral decision scenario.” The normalized values were evaluated together on a common graph. The region where the two curves converge or intersect was defined as the optimum value or value range that provides a balanced compromise between energy and economic criteria. This method represents a balanced design region obtained under the assumption of equal weighting.

2.4. Economic evaluation

The successful implementation of the wall system in buildings depends on its ability to operate with high efficiency, to establish a coherent architectural integration, and to be economically feasible. In this study, the economic evaluation was carried out based on payback period data. The payback period analysis is one of the most widely used methods in techno-economic assessment studies [31,44,45]. In this method, no ratio comparison is made; instead, the time interval required for the total cost to be recovered and for profit to begin is determined [46].

Accordingly, the annual energy cost must first be identified. The annual energy cost, C_y($), is equal to the sum of the annual heating energy cost, C_h($), and the annual cooling energy cost, C_c($).

$$C_{y=} C_h + C_c \tag{2}$$

The annual heating energy cost (C_h) was calculated using Eq. (3).

$$C_h = \frac{Q_{h,year}}{(H_u x \eta_k)} x C_f \tag{3}$$

Here, C_f represents the unit price of the fuel ($/m^3), H_u is the lower heating value of the fuel (kWh/m^3), and η_k is the overall efficiency of the heating system. The unit price and the lower heating value of the fuel used in these calculations were obtained from BOTAŞ [47] data. The annual cooling energy cost (C_c) was calculated using Eq. (4).

$$C_c = \frac{Q_{c,year}}{COP} x C_e \tag{4}$$

In this equation, C_e denotes the unit price of electricity ($/kWh) obtained from TÜİK [48] data, and the coefficient of performance (COP) of the cooling system was adopted from the study of Mangan and Oral [49].

The cost of the TIM-AG-PCM wall ($C_{\text{TIM–AG–PCM WALL}}$) was determined by multiplying the unit price obtained from the supplier by the corresponding surface area ($/m^2). Consequently, the total cost (C_T)—including the energy cost, the TIM-AG-PCM wall cost, and the standard wall cost—was calculated using Eq. (5).

$$C_T = (C_h + C_c) + C_{TIM-AG-PCM-WALL} \tag{5}$$

Here, C_h denotes the annual heating cost, C_c the annual cooling cost, and $C_{\text{TIM–AG–PCM WALL}}$ the cost of the proposed wall system. The payback period (years) was then calculated by dividing the cost of the transparent insulation latent heat storage wall $C_{\text{TIM–PCM WALL}}$ ($/m^2) by the annual fuel savings. The annual fuel savings (C_{afs}) were obtained by subtracting the annual energy cost of the dwelling with the transparent insulation latent heat storage wall C_{wd} ($/m^2) from that of the standard dwelling C_{sd} ($/m^2). The payback period was determined using Eqs. (6) and (7).

$$C_{afs=} C_{sd} - C_{wd} \tag{6}$$

$$PP = \frac{C_{TIM-AG-PCM}}{C_{afs}} \tag{7}$$

The payback period method employed for the economic evaluation of the transparent insulation latent heat storage wall has contributed to assessing the investment from an economic feasibility perspective.

3. Results

3.1. Experimental study

The analysis focused on temperature data collected from specific

measurement points in four experimental chambers: three chambers with TIM-AG-PCM walls of different configurations integrated into their south facades, and one reference chamber constructed with standard walls on all four facades. Experimental measurements were conducted to determine the thermal behavior of different TIM-AG-PCM wall configurations under atmospheric conditions during both summer and winter seasons. The measurement period covered a total of six months, including December, January, and February—representing the months when additional indoor heating was required—and July and August, representing the months when supplementary cooling was needed.

3.1.1. Heating season

Graphs prepared using real-time temperature data obtained from reference points in the experimental chambers during December, January, and February are presented in Fig. 6.

An examination of the temperature data collected from reference points during the heating season revealed that the TIM-AG-PCM wall types exhibited better thermal performance compared to the standard wall. Among the TIM-AG-PCM configurations, the lowest thermal performance was observed in the TIM-AG-PCM Wall Type-2. This was primarily due to the formation of convective air movements within the cavity when the ventilation covers were open during daytime hours. As a result of this air circulation, the brick surface facing the air cavity exhibited lower temperature values compared to the other TIM-AG-PCM wall types. When the covers were closed during the hours without solar radiation, air movement within the cavity was reduced, forming a stagnant air layer that limited heat transfer. This cyclic behavior decreased the amount of heat transferred to the PCM, restricting its activation process. Consequently, the temperature data obtained from the reference points of TIM-AG-PCM Wall Type-2 showed smaller increases compared to those of the standard wall, resulting in a more limited improvement trend.

TIM-AG-PCM Wall Type-1 demonstrated the highest thermal performance among the applications. The main reason for this was the presence of a narrow and stable air cavity, which effectively preserved the heat gained through radiation via the TIM layer. As a result, the temperature of the brick surface facing the air cavity increased, enabling more efficient heat transfer to the PCM layer. Consequently, the PCM operated effectively within the desired temperature range.

TIM-AG-PCM Wall Type-3 also exhibited high thermal performance, close to that of Wall Type-1. This was mainly because the curtain was kept open during the daytime to maximize the utilization of winter solar radiation. Thus, the heat gained through radiation was preserved within the insulated air cavity, increasing the inner brick surface temperature. During the hours when solar radiation decreased, closing the curtain limited heat transfer, allowing the PCM layer to activate more effectively.

Real-time temperature data obtained from thermocouples placed at the midpoint of the experimental chambers during December, January, and February were analyzed to assess the influence of the TIM-AG-PCM wall types on the mean radiant temperature (MRT). The corresponding graphs are presented in Fig. 7.

The graphs prepared from the MRT data recorded during the heating season show that the MRT values of Chambers 1, 2, and 3 were higher than those of Chamber 4, and that they exhibited a more damped response to fluctuations in outdoor air temperature. This indicates that, due to the thermal mass characteristics of PCM, the energy gained from solar radiation during daytime was stored and later released into the indoor environment with a delay, contributing to thermal comfort. The more stable and elevated MRT profiles observed throughout the day in Chambers 1 and 3, compared to the other chambers, further confirm the positive influence of PCM on indoor thermal conditions.

In Chamber 1, the 2 cm stagnant air gap in the TIM-AG-PCM wall acted as a thermal buffer, increasing the temperature of the wall's front surface and enhancing PCM activation. In Chamber 3, where the TIM-AG-PCM wall was installed on the south facade, the curtain was opened during daylight hours to admit solar radiation into the system, while during nighttime or low-radiation periods, the curtain was closed to reduce the overall heat transfer coefficient and to limit heat losses within the air gap.

In contrast, lower MRT values were recorded in Chamber 2 compared to the other experimental chambers with TIM-AG-PCM wall integration. In this configuration, the upper and lower ventilation covers on the wall's interior side were kept open during the day, allowing continuous convective air movement between the cavity and indoor air. Consequently, the front surface temperature of the wall remained lower than in the other applications. Although the closure of the air channels during evening hours enabled the air cavity to act as a partial thermal buffer, the daytime wall surface temperature did not reach the activation level required for the PCM. As a result, PCM performance was limited, and the chamber exhibited less improvement in indoor temperature compared to other configurations.

When all applications were compared, the reference chamber (Chamber 4) showed more abrupt and higher-amplitude MRT fluctuations in response to outdoor temperature variations. This finding indicates that conventional insulation systems are less effective in maintaining indoor thermal balance, whereas PCM-integrated wall systems provide a more stable and energy-efficient indoor environment.

Overall, the MRT data obtained during the heating season confirm that Chambers 1, 2, and 3 exhibited higher and more stable mean radiant temperatures compared to the reference Chamber 4. The consistent and elevated MRT profiles observed in Chambers 1 and 3 validate the stabilizing effect of PCM on indoor air temperature. The 2 cm air cavity in the TIM-AG-PCM wall integrated into the south facade of Chamber 1 acted as a thermal buffer zone, increasing the wall's inner surface temperature and facilitating effective PCM activation. Similarly, in Chamber 3, keeping the curtain open during daylight hours allowed solar radiation to enter the system, while closing it in low-radiation hours reduced the heat transfer coefficient and limited heat losses, ensuring that the PCM operated within its effective temperature range and enhanced the chamber's overall thermal performance.

Conversely, in Chamber 2, lower MRT values were recorded compared to the other TIM-AG-PCM wall configurations. The open position of the upper and lower vent covers during the day allowed for continuous convective airflow within the cavity, reducing the inner wall surface temperature and preventing the PCM from reaching its activation temperature. Although the cavity became partially stagnant during the night, insufficient daytime heat accumulation limited the PCM's contribution to indoor temperature stability.

When compared across all configurations, the reference chamber (Chamber 4) exhibited sharper and larger-amplitude MRT fluctuations in response to outdoor temperature variations. This outcome demonstrates that conventional wall systems are less effective in maintaining indoor thermal comfort, while PCM-integrated innovative wall solutions provide enhanced thermal stability and represent an effective passive design strategy.

3.1.2. Cooling season

Graphs prepared using real-time temperature data obtained from reference points in the experimental chambers during July and August are presented in Fig. 8.

An analysis of the temperature data collected from the reference points throughout the cooling season revealed that the TIM-AG-PCM Wall Types 2 and 3 exhibited lower temperature values and smaller fluctuation amplitudes compared to the Standard Wall. The performance levels of the TIM-AG-PCM walls varied depending on the specific design characteristics of each configuration.

In the TIM-AG-PCM Wall Type-1, the heat gained through radiation via the TIM layer was trapped within the narrow and stagnant air cavity due to its high insulation effect, leading to overheating of the outer wall surface. This caused unwanted heat transfer toward the interior during the cooling season, generating an additional thermal load and

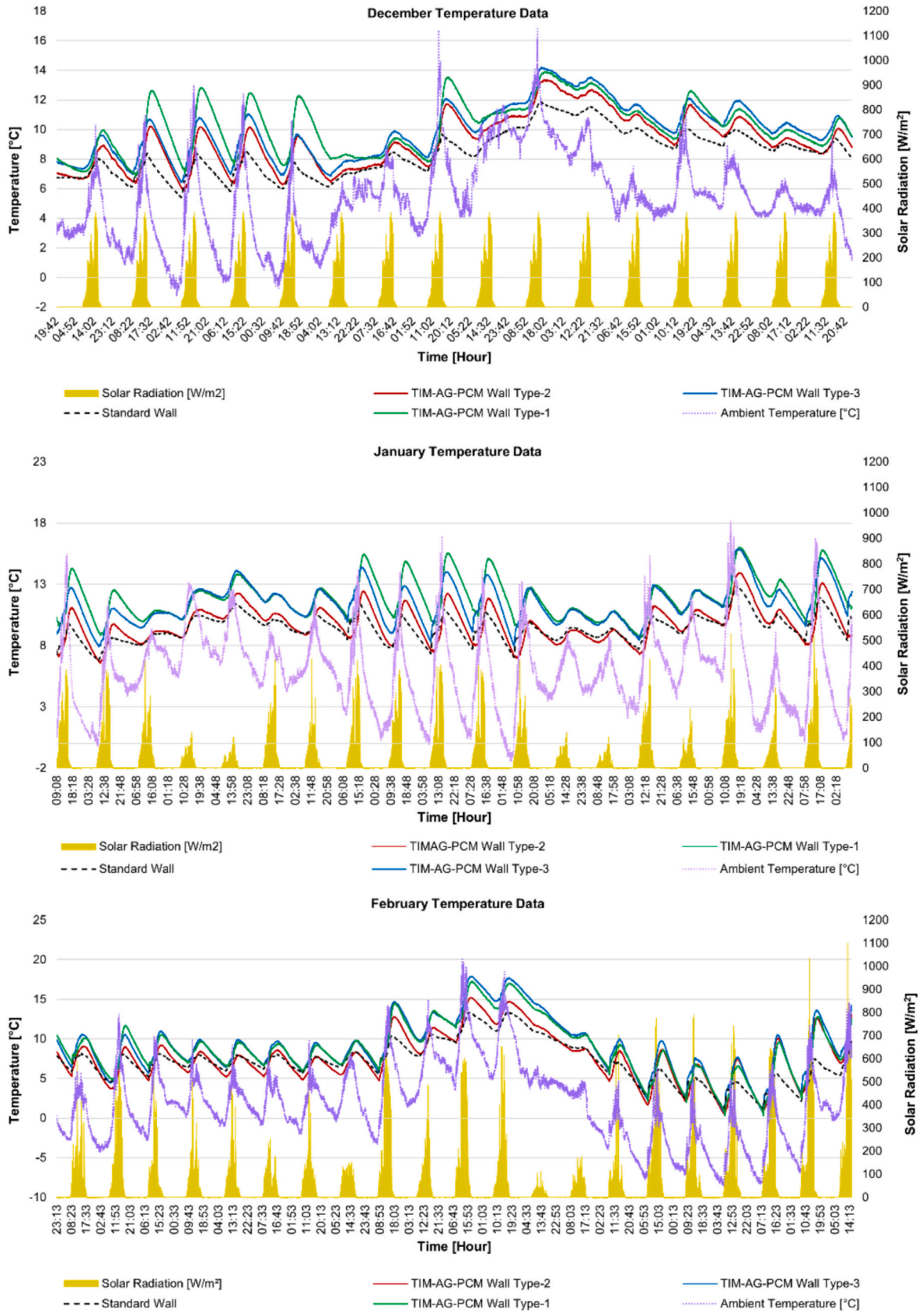


Fig. 6. Real-time measurement data of wall internal surface temperature, air temperature and solar radiation during the heating season.



Fig. 7. Real-time MRT data from the experimental chambers during the heating season.

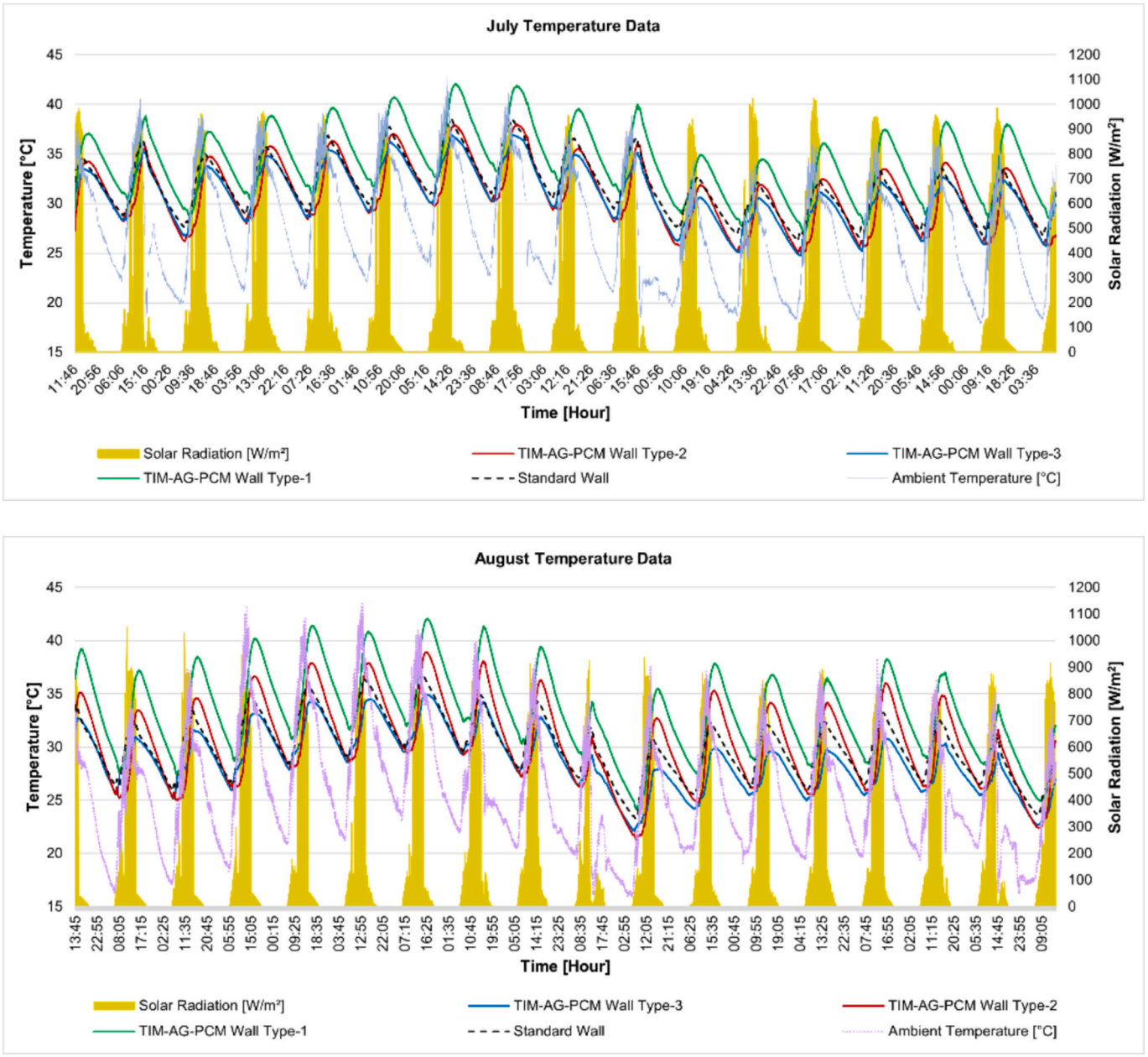


Fig. 8. Real-time measurement data of wall internal surface temperature, air temperature and solar radiation during the cooling season.

decreasing the wall's performance. Consequently, the Type-1 configuration exhibited the lowest performance during the cooling season, with higher measured surface temperatures than even the standard wall.

For the TIM-AG-PCM Wall Type-2, the lowest inner surface temperatures were obtained. During periods without solar radiation, opening the upper and lower air vents enabled convective air motion within the cavity, cooling the wall surface and allowing the PCM to operate within its effective temperature range. As a result, the PCM's heat storage and release capacity were enhanced, and the best thermal performance during the cooling season was achieved in this configuration.

The TIM-AG-PCM Wall Type-3 showed a similar inner surface temperature trend to Type-2 but exhibited the most stable thermal behavior in terms of temperature fluctuation amplitude. The shading element prevented the PCM-integrated surface from overheating during daytime, maintaining a more balanced wall inner surface temperature and suppressing sudden temperature increases. Consequently, the system provided an optimized thermal balance in terms of both heat gain control and continuity of indoor thermal comfort.

Real-time temperature data obtained from thermocouples placed at the midpoint of the experimental chambers during July and August were analyzed to evaluate the impact of the TIM-AG-PCM wall types on the mean radiant temperature. The corresponding graphs are presented in Fig. 9.

The MRT data obtained during July and August clearly reveal the influence of the TIM-AG-PCM wall systems on indoor thermal comfort during the cooling season. Overall, the integration of TIM and PCM contributed to more balanced thermal behavior by reducing indoor temperature fluctuations, although the level of performance varied significantly depending on the system configuration.

Chamber 1 recorded the highest MRT values during daytime in both months, indicating the lowest performance in terms of cooling effectiveness. This behavior was attributed to the excessive heat accumulation in front of the wall, caused by the trapping of radiative heat within

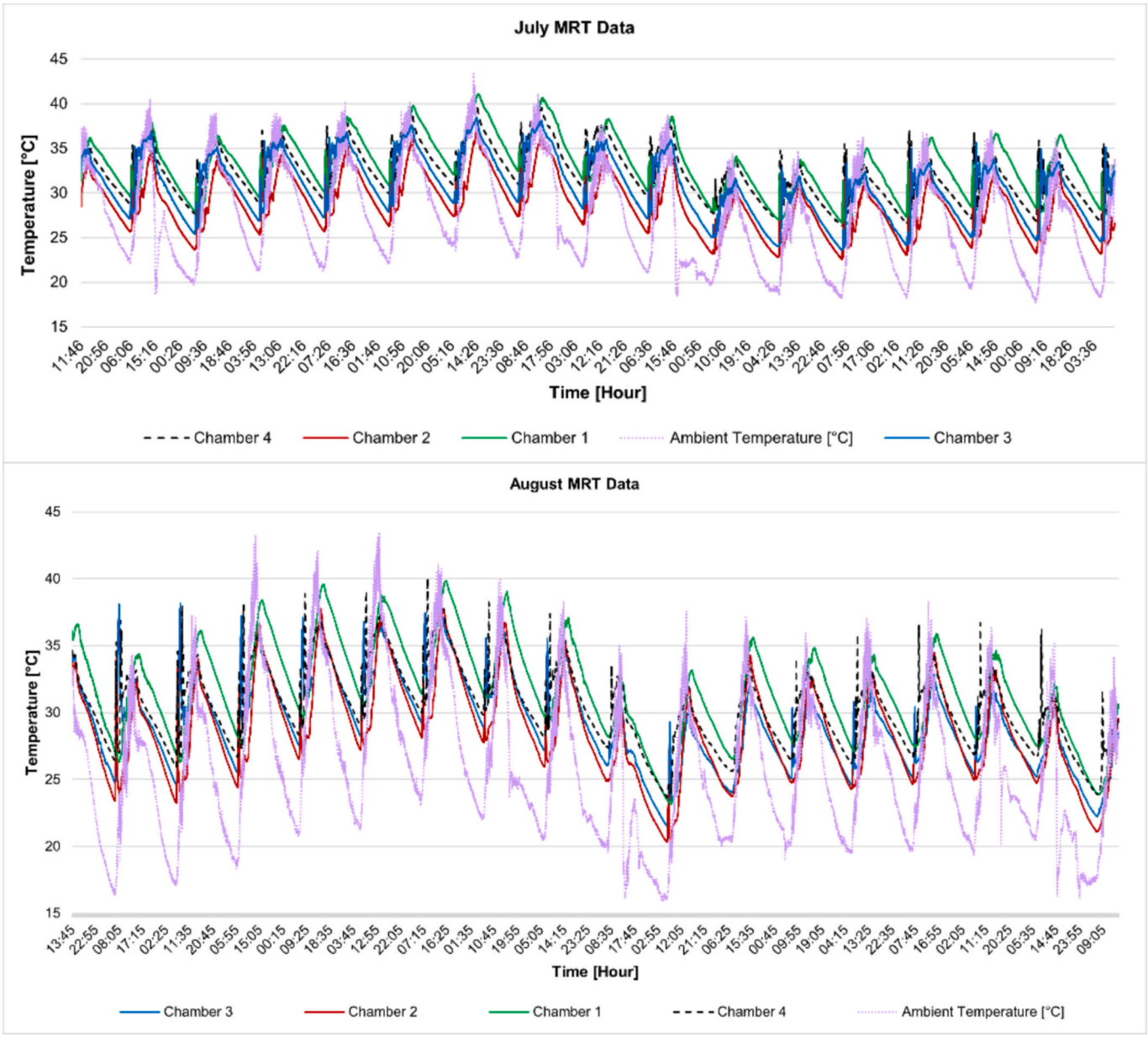


Fig. 9. Real-time MRT data from the experimental chambers during the cooling season.

the narrow and stagnant air gap between the TIM and PCM layers. This overheated zone prevented the PCM from reaching its effective phase-change temperature, keeping it in a constant molten state. As a result, the PCM could not undergo phase transition and thus failed to provide cooling benefits, making Chamber 1 the least effective among the test chambers.

Chamber 2 demonstrated the most stable and lowest MRT values during the cooling season. Keeping the ventilation openings at the upper and lower parts of the thermal wall open allowed natural convection currents to develop within the cavity. This air movement prevented excessive surface heating on the exterior side of the wall and supported effective PCM operation. Consequently, PCM underwent regular phase transitions, maintaining indoor temperatures closest to the comfort range and resulting in the most efficient cooling performance.

Chamber 3 generally exhibited thermal performance comparable to that of Chamber 2, though it displayed the most stable temperature fluctuations. The shading element limited solar radiation during daytime, preventing overheating of the PCM-integrated surface and maintaining controlled inner surface temperatures. However, because of the stagnant air layer within the cavity, the heated air did not circulate, leading to a certain degree of heat accumulation in front of the wall and slightly higher MRT values compared to Chamber 2.

Chamber 4, in contrast, responded more rapidly and with higher amplitude to variations in outdoor air temperature than the chambers equipped with TIM-AG-PCM systems. This finding indicates that conventional insulation systems fail to sustain temporary indoor thermal balance and exhibit a thermal response highly dependent on outdoor conditions.

When the data obtained for both heating and cooling seasons were compared, it was observed that the TIM-AG-PCM wall on the south facade of Chamber 1 performed best during the heating season. However, during the cooling season, the thermal behavior of the system reversed and showed a different performance pattern. Examination of the cooling season results revealed that TIM-AG-PCM Wall Type-2 achieved the lowest inner surface temperature. Although the chamber equipped with this wall (Chamber 2) recorded the lowest MRT value, its

response to outdoor temperature fluctuations was faster and of higher amplitude compared to the TIM-AG-PCM Wall Type-3, which had a less desirable effect on comfort.

The most noteworthy configuration in both seasons was the TIM-AG-PCM Wall Type-3. During summer, it reduced the wall's inner surface temperature by approximately 2 °C compared to the standard wall, providing a cooling effect, while during winter, it increased the temperature by about 3 °C. Thus, it exhibited balanced and enhanced performance across both heating and cooling seasons. The influence of this configuration on indoor comfort—an important criterion for energy-efficient design—was consistently positive in both periods. The MRT data for both seasons showed narrower amplitude and more stable trends, confirming its ability to maintain thermal stability. Therefore, for building energy performance analyses, the TIM-AG-PCM Wall Type-3, which demonstrated the best performance in experimental measurements, was selected.

3.2. Simulation

For the purpose of comparing the data obtained for the heating and cooling seasons, the reference residential building was defined proportionally as "0%." For both seasons, the performance results of the TIM-AG-PCM Wall Type-3 were obtained for each percentage level, increasing from 20% to 100% on each facade in 20% increments. To enable comparison of the obtained results, the reference building was proportionally defined as "0%" (Fig. 10).

3.2.1. South facade

The impact of the TIM-AG-PCM Wall Type-3 integrated into the south facade on building performance during the heating season was evaluated through heating load and operative temperature analyses for December, January, and February (Fig. 11).

The graph of total heating load (Fig. 11) shows that as the proportion of the TIM-AG-PCM Wall Type-3 decreases, the heating load increases noticeably. In December, under the 100% application scenario, the heating load was approximately 1000 kWh, whereas under the 0% application scenario, it approached 1250–1300 kWh, corresponding to an increase of roughly 25–30%. A similar increasing trend was observed in January and February, indicating that higher facade coverage of the TIM-AG-PCM Wall Type-3 effectively reduces heat losses and improves seasonal energy performance. According to the operative temperature analysis, increasing the proportion of the TIM-AG-PCM Wall Type-3 results in a more stable indoor temperature profile and reduces the rate of temperature decline. Under the 100% application scenario, the average operative temperature remained approximately within the range of 18.8–19 °C, supporting indoor thermal comfort during the heating period.

The cooling season analyses indicate (Fig. 12) a noticeable reduction in cooling load as the proportion of the TIM-AG-PCM Wall Type-3 increases. In the 100% application scenario, the cooling load in June was approximately 350 kWh, while in the 0% application, it exceeded 600 kWh, an increase of nearly 70%. A similar pattern was observed in July and August, indicating that the TIM-AG-PCM Wall Type-3 configuration limited solar gains by maintaining the shading element in a closed position during hours of intense solar radiation and in an open position during evening hours with reduced solar exposure. This dynamic operation effectively lowered the thermal load. According to the operative temperature analysis, as the proportion of the TIM-AG-PCM Wall Type-3 decreases, the indoor temperature rises; while the average temperature in the 100% application was approximately 25 °C, it reached around 27 °C at the 20% application level.

3.2.2. West facade

The impact of the TIM-AG-PCM Wall Type-3 integrated into the west facade on building performance during the heating season was evaluated based on the graphs presented in Fig. 13.

An examination of the heating season analysis graphs for the west facade (Fig. 13) indicates that, under the 100% application scenario, an energy saving of approximately 300–400 kWh was achieved in all months compared to the 0% application. This finding demonstrates that the integration of the TIM-AG-PCM Wall Type-3 on the west facade effectively reduces heat losses and enhances the building's overall energy efficiency. According to the operative temperature analysis, as the proportion of the TIM-AG-PCM Wall Type-3 increases, indoor temperatures remain more stable. In February, an average temperature of approximately 19.5 °C was achieved under the 100% application, while this value dropped to around 18.5 °C under the 0% application scenario.

The analysis results illustrating the effects of the TIM-AG-PCM Wall Type-3 ratio on cooling load and operative temperature for the west facade are presented in Fig. 14.

The graphs corresponding to the cooling season show that, in June, there was a difference of approximately 200 kWh between the 100% and

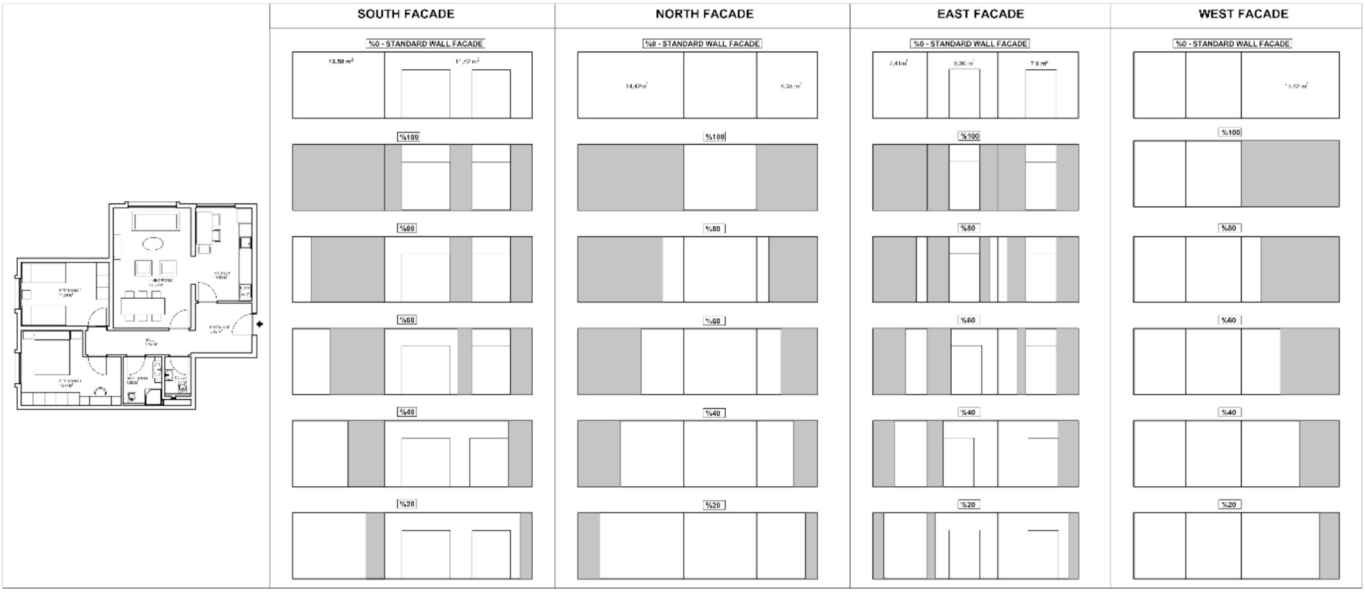


Fig. 10. Layout of the TIM-AG-PCM Wall Type-3 according to the presence rate on four facades.

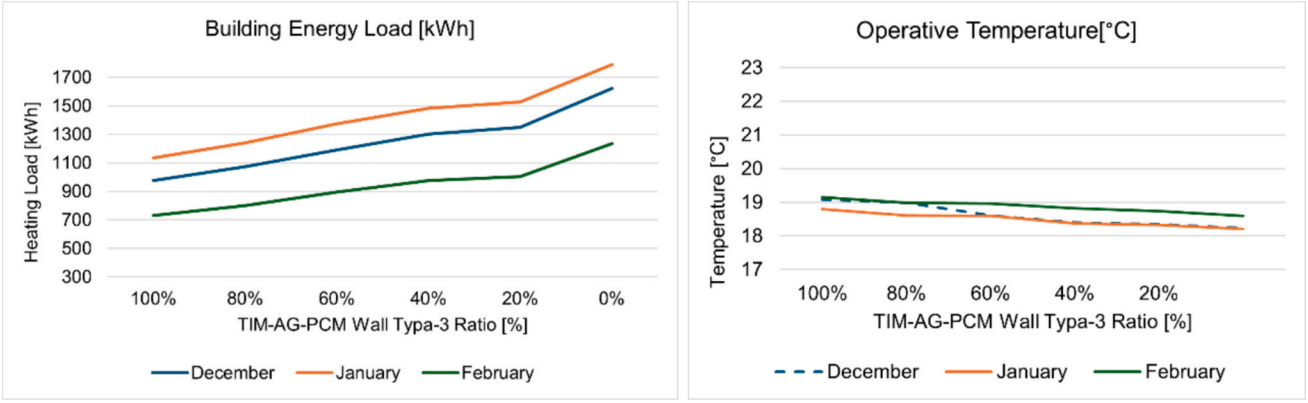


Fig. 11. Heating season TIM-AG-PCM Wall Type-3 ratios building energy load and operating temperature analyses.

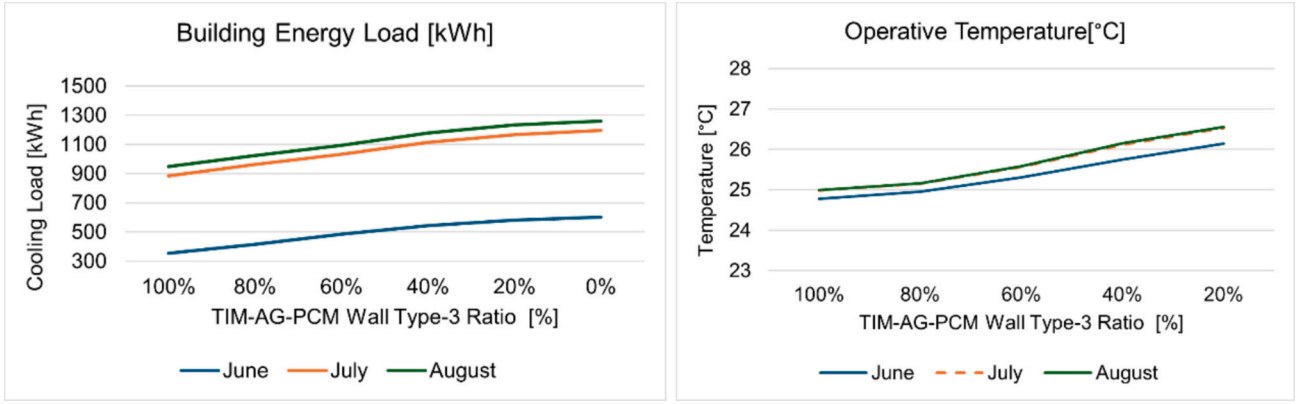


Fig. 12. Cooling season TIM-AG-PCM Wall Type-3 ratios building energy load and operating temperature analyses.

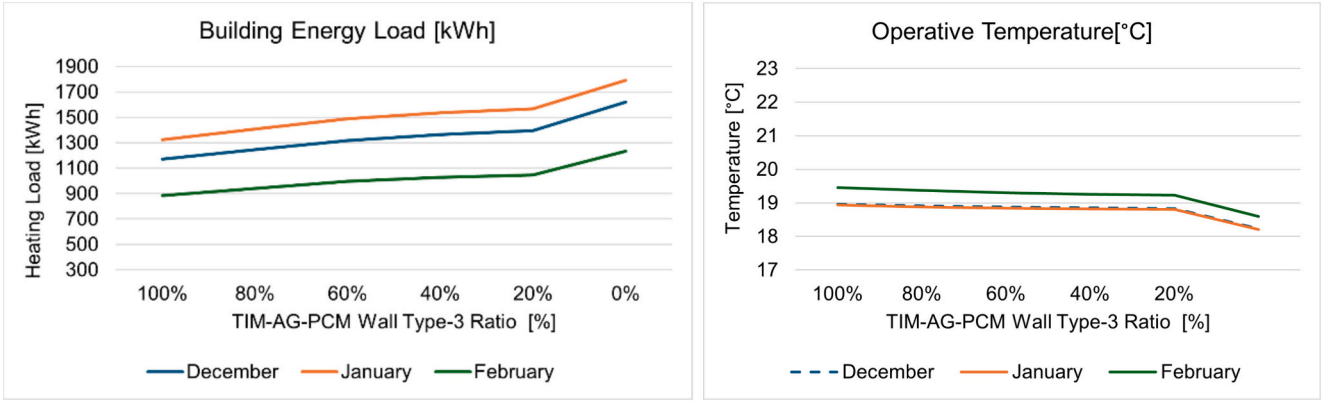


Fig. 13. Building energy load and operative temperature analyses based on TIM-AG-PCM Wall Type-3 ratio for west facade heating season.

0% applications of the TIM-AG-PCM Wall Type-3 on the facade. According to the operative temperature graphs, as the proportion of the TIM-AG-PCM Wall Type-3 decreases, indoor temperatures increase: under the 100% application, the average temperature remained around 25 °C, while under the 0% application, it reached approximately 26 °C.

3.2.3. North facade

The analysis results for the heating season, based on the ratios of the TIM-AG-PCM Wall Type-3 integrated into the north facade, are presented in Fig. 15.

An examination of the graphs for the heating season (Fig. 15) shows that under the 100% application scenario, the heating load in January was approximately 1300 kWh, whereas in the 0% application, it increased to around 1800 kWh. Similar increases were also observed in December and February. Although the north facade does not receive direct solar radiation, these results indicate that the thermal insulation effect provided by the TIM-AG-PCM Wall Type-3 significantly reduced heat losses. According to the operative temperature analysis, at 100% application, the indoor temperature was maintained around 19 °C, whereas at 0% application, it dropped below 18 °C. This demonstrates that even on the north facade, where solar gains are minimal, the TIM-AG-PCM Wall Type-3 reduces heating loads and enhances indoor temperature stability, contributing to occupant comfort.

An evaluation of the cooling season performance of the TIM-AG-PCM

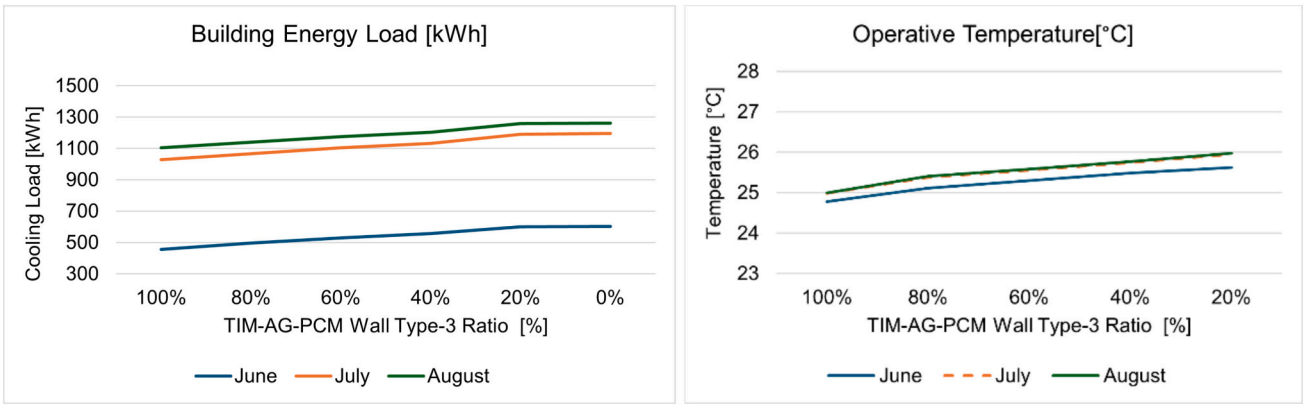


Fig. 14. Building energy load and operative temperature analyses based on TIM-AG-PCM Wall Type-3 ratio for west facade cooling season.

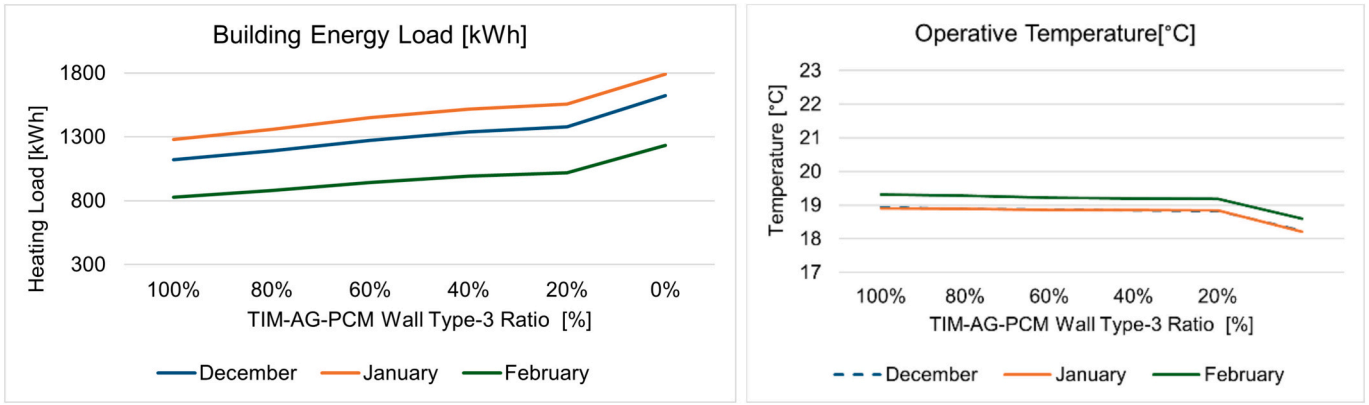


Fig. 15. Building energy load and operative temperature analyses based on TIM-AG-PCM Wall Type-3 ratio for north facade heating season.

Wall Type-3 on the north facade, based on the analysis results in Fig. 16, indicates that the difference between the 100% and 0% applications was approximately 100 kWh in June, while this difference decreased further in July and August. This outcome shows that, since the north facade is not directly exposed to solar radiation, the contribution of the TIM-AG-PCM Wall Type-3 to reducing cooling load remains limited. However, according to the operative temperature graphs, as the proportion of the TIM-AG-PCM Wall Type-3 decreases, the indoor temperature rises. Under the 100% application, the indoor temperature was maintained at approximately 25 °C, while under the 0% application, it approached 26 °C. This difference is primarily associated with the ability of the TIM-AG-PCM Wall Type-3 to slow down heat transfer and stabilize indoor temperature fluctuations, rather than reducing direct heat gains. In conclusion, on the north facade, the effect of the TIM-AG-PCM Wall Type-3 during the cooling season is more oriented toward improving thermal comfort rather than achieving direct energy savings.

3.2.4. *East facade*

The analysis results for the heating season, based on the ratios of the TIM-AG-PCM Wall Type-3 integrated into the east facade, are presented in Fig. 17.

As shown in Fig. 17, under the 100% application scenario, the building heating load in January was approximately 1300 kWh, whereas in the 0% application, it reached about 1700 kWh, indicating an increase

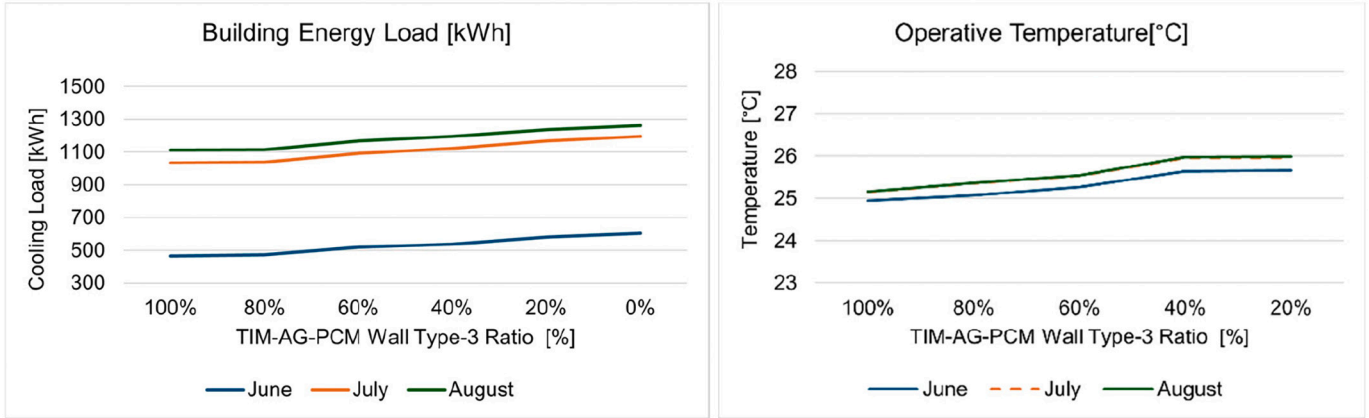


Fig. 16. Building energy load and operative temperature analyses based on TIM-AG-PCM Wall Type-3 ratio for north facade cooling season.

of over 30%. This demonstrates that the TIM-AG-PCM Wall Type-3, applied on the east facade exposed to solar radiation during the morning hours, effectively limited heat losses and contributed to passive heat gains in the early part of the day. The operative temperature data support this finding, showing that under the 100% application, indoor temperatures remained in the range of 18.8–19 °C, while under the 0% application, the temperature in all months fell below 18 °C. Even when the TIM-AG-PCM Wall Type-3 covered only 20% of the facade, it provided approximately 14% energy savings compared to the standard wall during January—the coldest month of the heating season—and increased the operative temperature by 0.5 °C.

The analysis results for the cooling season, based on the ratios of the TIM-AG-PCM Wall Type-3 integrated into the east facade, are presented in Fig. 18.

An examination of the cooling season graphs (Fig. 18) shows that in June, the cooling load was approximately 500 kWh under the 100% TIM-AG-PCM application, whereas it exceeded 600 kWh under the 0% condition—an increase of nearly 20%. Similarly, in July and August, the energy load for the 100% application was approximately 1000–1050 kWh, while in the 0% application, the cooling load was about 200 kWh higher. According to the operative temperature evaluation, under the 100% TIM-AG-PCM Wall Type-3 application, indoor temperatures remained stable between 25.6 and 25.8 °C, whereas under the 0% condition, temperatures approached 26.0 °C, showing an increase of approximately 0.3–0.4 °C. Even when the TIM-AG-PCM Wall Type-3 was applied to only 20% of the east facade, although there was a slight increase in energy load and temperature values, the overall building energy performance improved compared to the standard wall.

3.3. Sensitivity analysis results

For the calculation of the payback period of the TIM-AG-PCM Wall Type-3 applied to all four facades in 20% increments, both the initial investment cost and the operational cost were determined. To identify the cost per square meter of the TIM-AG-PCM Wall Type-3 and the standard wall, a comparative cost analysis was conducted. The results of this cost study, based on data obtained from the manufacturer, are presented in Table 4.

Following the building energy performance analysis, the cost-effectiveness evaluation of the TIM-AG-PCM Wall Type-3—applied to each facade in increments of 20% within the 20–100% range—was conducted by comparing the normalized data of the payback period (initial investment cost/operational cost) and the total energy performance for each application ratio. To enable this comparison, the payback period data and performance data, which were measured on different scales, were normalized using the min–max normalization method, converting the dataset into a 0–1 range for graphical comparison (Fig. 19).

When the normalized total energy load and payback period values of the TIM-AG-PCM Wall Type-3 were comparatively analyzed for the different application ratios across the four building facades, it was observed that the relationship between energy performance and economic return varied significantly depending on facade orientation.

The south facade, due to its high solar radiation potential, emerged as the most advantageous orientation in terms of energy efficiency. As the proportion of the TIM-AG-PCM Wall Type-3 increased, the total energy load decreased, reaching its minimum under the 100% application. However, because of the high initial investment cost, the payback period in this case exceeded the building's expected service life. The graphs indicate that the optimum value providing a trade-off solution between energy performance and payback period occurs within the 35–40% range.

For the north facade, although direct solar gains are limited, the TIM-AG-PCM Wall Type-3 wall system reduced total heating load by approximately 18% through its thermal insulation effect. Conversely, as the application ratio decreased, the payback period shortened non-linearly, revealing an inverse relationship between energy efficiency and return on investment. The 50% ratio, at which the graphical curves converge most closely, is considered the optimum value for the north facade, representing the trade-off solution between energy performance and payback period.

For the east facade, the results reflect the influence of morning solar radiation on passive heat gain. As the proportion of the TIM-AG-PCM Wall Type-3 increased, the total energy load decreased, reaching a minimum under the 100% application. However, at these ratios, the payback period increased considerably. Conversely, reducing the application area lowered the total cost and shortened the payback period. The 50–60% range, where the total energy load and payback period curves converge most closely, is considered the optimum range for the east facade, representing the trade-off solution between energy performance and payback period.

The west facade, exposed to high afternoon solar gains, exhibited the most pronounced effectiveness of the TIM-AG-PCM Wall Type-3 system in reducing both heating and cooling loads. As the application ratio increased, the total energy load consistently decreased, reaching the lowest value at 100% application. However, the payback curve showed a sharp decline beyond the 60% level, reaching its minimum around the 20% application. This indicates that while reducing the investment area significantly lowers cost, the corresponding decrease in energy savings is not directly proportional. Therefore, an application ratio of 50–60% on the west facade is considered the optimum value, representing the trade-off solution in terms of both energy savings and payback period.

4. Discussion

To comprehensively examine the architectural applicability, energy

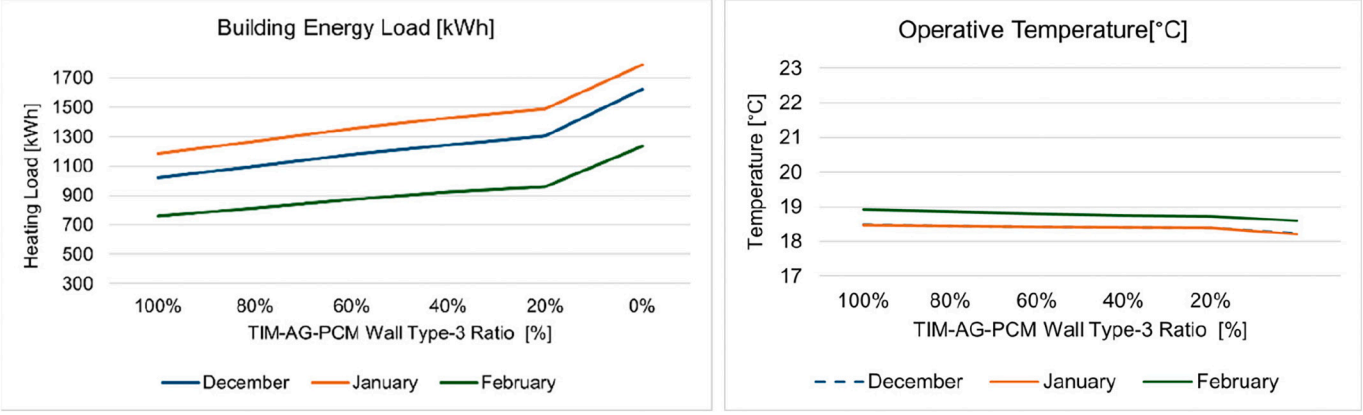


Fig. 17. Building energy load and operative temperature analyses based on TIM-AG-PCM Wall Type-3 ratio for east facade heating season.

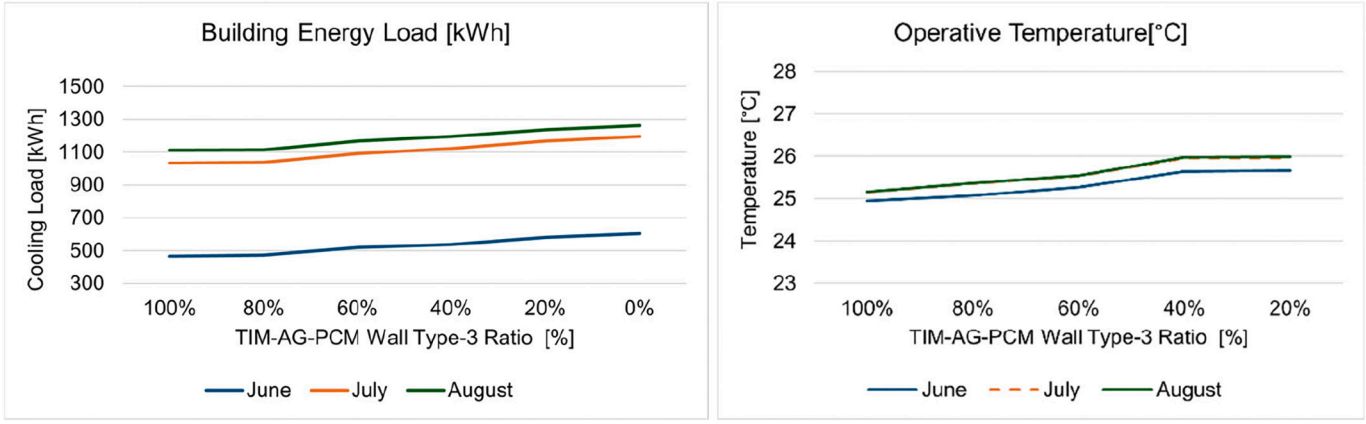


Fig. 18. Building energy load and operative temperature analyses based on TIM-AG-PCM Wall Type-3 ratio for east facade cooling season.

Table 4
Cost per square meter of standard wall and TIM-AG-PCM Wall Type-3.

	Material	Usage per m^2	Unit cost (per m^2)
TIM-AG-PCM Wall Type-3	4 mm single glass	Two 1 m × 1 m glass panels	907,32 Euro
	Cabot LA1000 (aerogel)	10 l	
	Plaster	1 m^2 area	
	Clay brick	39 pcs	
	RT18HC/RT22HC (PCM)	39 unit	
	Paint	1 m^2 area	
Standard wall	Paint	1 m^2 area	41,86 Euro
	Plaster	1 m^2 area	
	XPS insulation	Two 100 × 200 cm panels	
	Hallow brick	18 pcs (19 cm × 29 cm × 13.5 cm)	

efficiency, and economic return potential of the TIM-AG-PCM Wall Type-3 within architectural integrity, the findings were discussed under three main themes: design, performance, and cost. Under the design heading, the architectural and structural implications of the wall system were examined in relation to its physical components, facade orientation, and application ratios. The performance section focused on evaluating the system's thermal response based on indoor and surface temperatures as well as energy loads. The cost discussion addressed the payback period of the system in relation to its application area and energy-saving potential. This multidimensional analysis aims to holistically reveal the applicability, energy efficiency, and economic return potential of the TIM-AG-PCM Wall Type-3 within an integrated architectural framework, thereby providing guidance for future design and decision-making processes.

4.1. Design

In this study, the high thermal insulation capacity offered by the TIM, along with its high solar radiation transmittance, and the latent heat storage ability provided by the PCM through phase change were evaluated as complementary components that enhance the system's

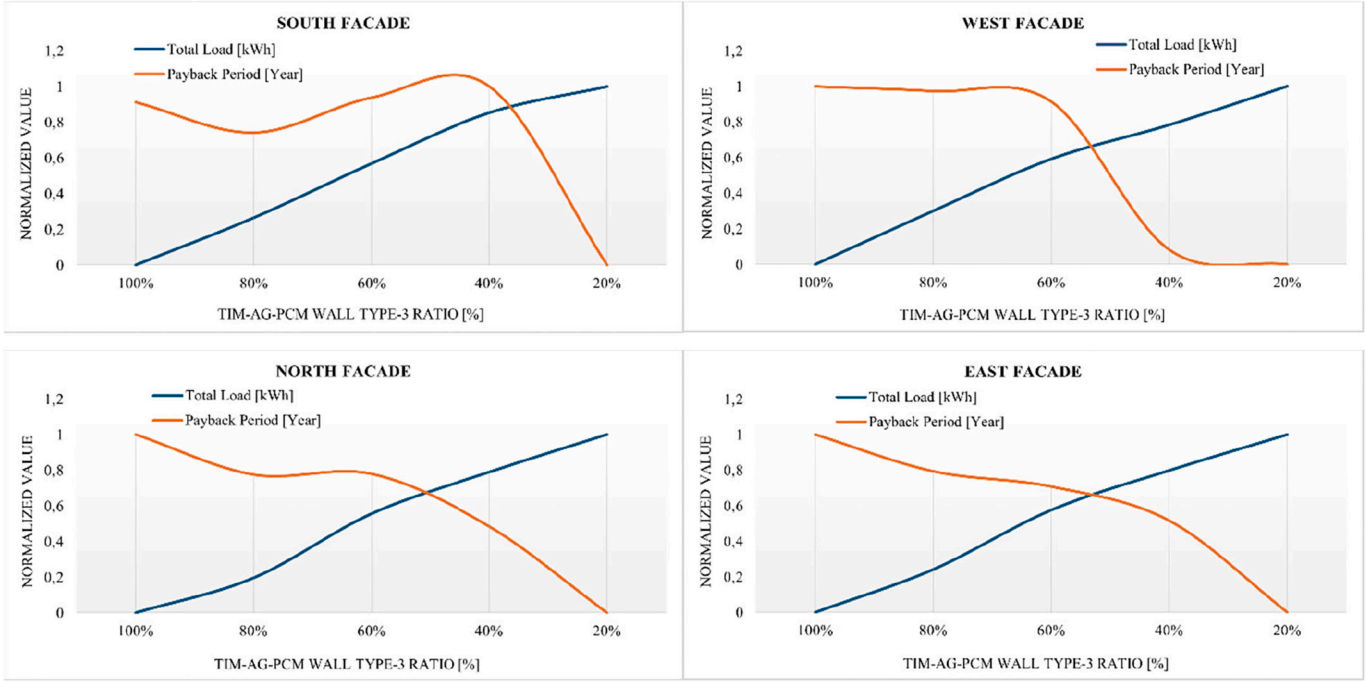


Fig. 19. Total load and payback season change depending on the presence rate of TIM-AG-PCM Wall Type-3 on all facades.

performance during the heating season. Experimental studies conducted under the climatic conditions of Ankara confirmed, through building-scale energy simulations, that the TIM-AG-PCM Wall Type-3 demonstrated the highest performance in both the heating and cooling seasons. This wall type stands out as an effective implementation of climate-responsive passive design strategies.

The analyses revealed that applying the TIM-AG-PCM Wall Type-3 at varying ratios on different facades produced optimum results in terms of both energy and economic efficiency. At the building scale, the optimal application ratios were determined as 35–40% for the south facade, 50% for the north facade, and 50–60% for the east and west facades. These results indicate that the system should not be applied uniformly across all facades but rather in varying proportions depending on solar orientation and heat-gain potential.

Facade-based analyses showed that although the south facade had the lowest application ratio (≈38%), this proportion provided the most balanced performance by reducing cooling loads in summer and optimizing heat gains in winter. The higher-than-expected optimum ratio for the north facade was associated with the system's low U-value, which minimizes heat losses and contributes passively to solar gains in winter. The east and west facades benefited from greater exposure to morning and afternoon sunlight, enhancing the effectiveness of PCM in winter while also maintaining favorable energy performance under lower summer radiation levels. This behavior reduced operating costs and shortened the payback period, indicating that higher application ratios on the east and west facades represent the most effective solution for energy efficiency. Furthermore, the selection of PCM materials suitable for the specific climatic conditions proved to be a decisive factor influencing performance. The analyses for Ankara's climate demonstrated that the hybrid integration of RT18HC (for the heating season) and RT22HC (for the cooling season) PCMs at a 50% ratio provided a balanced thermal response throughout the year.

Overall, these findings confirm that the TIM-AG-PCM wall system is not merely a building component enhancing energy efficiency, but a holistic design solution that can be sensitively adapted to climate, orientation, and architectural design decisions.

4.2. Performance

Under the climatic conditions of Ankara, experimental measurements showed that the TIM-AG-PCM Wall Type-3 exhibited approximately 18% higher thermal performance during the heating season and 5% higher performance during the cooling season compared to the standard wall. The highest and lowest inner surface temperatures recorded in December and July are presented in Table 5.

Facade-based building-scale energy performance analyses revealed that the application of the TIM-AG-PCM Wall Type-3 reduced energy loads in all orientations and maintained operative temperatures within the comfort range. On the south facade, the 100% application achieved average temperatures of approximately 19 °C in winter and 25 °C in summer. On the east facade, morning solar gains reduced heating loads, while the 100% application achieved 100–150 kWh of cooling energy savings. On the west facade, up to 200 kWh of energy savings were observed due to the afternoon solar radiation effects. Even on the north facade, despite limited solar exposure, heat losses decreased and operative temperatures improved by approximately 1 °C.

Table 5
Temperature values recorded on the inner surface of standard wall and TIM-AG-PCM Wall Type-3 during December and July.

	TIM-AG-PCM Wall Type-3		Standard wall	
	Min. temp. [°C]	Max. temp. [°C]	Min. temp. [°C]	Max. temp. [°C]
Heating season	6.42	14.20	5.42	11.85
Cooling season	24.77	36.90	26.24	38.60

When the mathematical analysis results of Bilgin and Arıcı [50] for a PCM-integrated wall model are compared with the experimental data of the TIM-AG-PCM Wall Type-3 (Table 5), it is observed that the integration of TIM and aerogel nearly doubled performance by achieving approximately 1.5 °C lower inner surface temperatures during the heating season and 2 °C lower temperatures during the cooling season. This improvement is attributed to the high insulation property of the aerogel and the semi-transparency of the TIM, which supports the phase change process of the PCM.

Furthermore, when compared with the PCM–pumice block study conducted by Saylam Canım [51] (Table 6), the TIM-AG-PCM Wall Type-3 demonstrated 43% higher performance during the heating season and 31% higher performance during the cooling season. This difference is primarily due to the hybrid structure of the system, which integrates two PCM materials suitable for both summer and winter conditions in equal proportions, and the shading element that limits excessive radiation effects.

In this context, integrating two PCMs with different melting temperatures (RT18HC and RT22HC) into the TIM-AG-PCM wall system extends the effective phase change temperature range and enables a staged latent heat storage mechanism under varying seasonal conditions. Due to their different melting temperatures, these two PCMs do not thermally interfere with each other; instead, they operate in a complementary, sequential manner. Each PCM becomes active within a specific temperature interval, thereby preventing overlapping phase transitions.

When the seasonal performance is examined, increased solar radiation during summer raises the temperature within the wall section above the melting points of both PCMs, allowing latent heat to be stored during daytime. As temperatures decrease, RT22HC, with its higher melting temperature, solidifies first and releases the stored heat, followed by RT18HC at lower temperatures, resulting in a gradual release of heat. During the winter period, a heat storage–release cycle dominated by RT18HC, which has a lower activation temperature, is observed. During transitional seasons, this sequential phase-change behavior provides extended thermal buffering, reducing indoor temperature fluctuations and enhancing thermal stability.

Considering the implications of this physical mechanism at the building scale, the conducted sensitivity analyses indicate that applying TIM-AG-PCM Wall Type-3 at ratios of 35–40% on the south facade, 50% on the north facade, and 55–60% on the east and west facades offers the most suitable range for reducing annual energy demand and improving cost efficiency. At these application levels, the system achieved energy savings of 26% during the heating season and 10% during the cooling season compared to the reference building with standard walls (0% TIM-AG-PCM Wall Type-3), while maintaining a stable and high level of thermal performance throughout the year.

4.3. Cost

The key factor in the economic evaluation of the TIM-AG-PCM wall system is the long payback period, which results from its high initial investment cost. Since the production and application costs of the TIM and PCM components are higher than those of conventional insulation materials, the system's initial cost increases, thereby extending the payback period. Particularly at 100% application ratios, the cost escalation associated with surface area expansion exceeds that of a standard wall, prolonging the economic return period.

Nevertheless, both experimental and simulation findings demonstrate that the TIM-AG-PCM Wall Type-3 provides significant reductions in energy loads during both the heating and cooling seasons. The system offers high energy savings and sustained thermal comfort, as it passively transmits solar radiation and releases the heat stored in the PCM during nighttime, thereby reducing temperature fluctuations. This mechanism

Table 6
Comparison of the performance of the TIM-AG-PCM Wall Type-3 with the study.

	Heating season			Cooling season		
	December [kWh]	January [kWh]	February [kWh]	June [kWh]	July [kWh]	August [kWh]
PCM-pumice blocks wall	2417.52	2538.44	1493.4	876.74	1647.94	1480.31
TIM-AG-PCM Wall Type-3	1276	1454.12	952.51	517.6	1088.87	1158.83

generates a long-term economic benefit that offsets the high initial investment cost over time.

Advancements in material technologies and the sensitivity analysis of production processes have the potential to significantly reduce the cost per square meter and the overall payback period. Furthermore, government incentives and the use of alternative raw materials could strengthen the economic feasibility of this innovative wall system.

Another important parameter in the cost assessment of the TIM-AG-PCM wall system is maintenance and repair requirements. The long-term thermal stability of the materials used throughout the building's life cycle directly affects this parameter. Accelerated thermal cycling tests conducted by Katish et al. [52] confirmed that RT18HC and RT22HC PCMs maintained stable phase-change temperatures after 10,000 cycles, while Novik [53] reported that granular aerogel exhibited only a 1–4% increase in U-value after an equivalent of 20 years of aging. These findings indicate the long-term thermal stability and low maintenance requirements of the TIM and PCM components.

In conclusion, although the high initial investment cost currently limits the widespread adoption of the system, enhanced energy efficiency, low operational costs, and long-lasting thermal durability make the TIM-AG-PCM wall system a sustainable solution that achieves an effective balance between performance and cost over the long term.

5. Conclusions

In this study, an innovative passive building component defined as the TIM-AG-PCM wall system was developed, and experimental analyses were conducted for different configurations. According to the findings, TIM-AG-PCM Wall Type-3 demonstrated approximately 18% higher performance during the heating season and 5% higher performance during the cooling season compared to the standard wall. Building-scale analyses indicated that the implementation of the system reduced annual total energy consumption by 28.24%. This improvement is attributed to the semi-transparent structure of the TIM, which facilitates solar radiation transmission and supports the phase-change process of the PCM, as well as to the low thermal conductivity of the aerogel material, which limits heat losses.

From a design perspective, the ability to apply the wall system at variable ratios on different facades provides significant flexibility. Sensitivity analyses indicated that application ratios of 35–40% on the south facade, 50% on the north facade, and 50–60% on the east and west facades represent a trade-off solution between energy performance and payback period. At these ratios, building energy consumption decreased by 25.8% compared to the standard wall. Furthermore, the hybrid use of two PCMs with different melting temperatures contributed to performance continuity not only during the heating and cooling seasons but also during transitional periods through staged phase-change behavior.

One of the limitations of the study is that the analyses were conducted under the climatic conditions of Ankara. Performing similar analyses in different climate regions may lead to variations in the most suitable TIM-AG-PCM wall configuration for each region. The operating temperature of the PCM integrated into the wall body and its application ratio within the wall assembly are expected to vary depending on regional climatic characteristics. Consequently, the facade-specific optimal application ratios of the TIM-AG-PCM wall may also differ, necessitating region-specific design decisions.

Another limitation is that the building energy performance analyses were carried out for a single-storey residential building model. In multi-storey buildings or structures with different usage types, the thermal behavior of the TIM-AG-PCM wall may vary due to parameters such as internal heat gains, inter-zonal airflows, and complex thermal mass interactions.

Additionally, the thermal performance of the TIM-AG-PCM wall under real climatic conditions was evaluated based on surface temperature data. Assessing PCM charge–discharge behavior from surface temperatures rather than direct heat-flux measurements led to interpreting the energy storage–release process using relative performance indicators rather than absolute quantitative values. This limitation is primarily due to the absence of direct heat-flux measurements, as heat-flux sensors were not used in the experimental setup. Moreover, energy performance and payback period data were normalized using a minimum–maximum scaling approach, and both criteria were given equal weight. This approach enabled the identification of facade-specific optimum ratios under defined assumptions.

In conclusion, the TIM-AG-PCM wall system can be regarded as a passive building component adaptable to climate, orientation, and architectural design parameters. Future studies involving parametric and regional analyses for different PCM ratios and climatic conditions are expected to contribute to a more comprehensive evaluation of the system's applicability and cost-effectiveness. Furthermore, applying multi-criteria decision-making methods to determine facade-specific optimal application ratios would enable a more robust optimization framework that better reflects decision-maker preferences.

CRediT authorship contribution statement

Cansu Bekler: Writing – original draft, Visualization, Validation, Software, Data curation. **İdil Ayçam:** Writing – review & editing, Supervision, Project administration, Funding acquisition, Conceptualization. **Mustafa Zeki Yılmazoğlu:** Writing – review & editing, Visualization, Software, Methodology, Investigation. **Asena Soyluk:** Validation, Methodology, Investigation, Formal analysis, Conceptualization.

Declaration of competing interest

The authors declare the following financial interests/personal relationships which may be considered as potential competing interests: Idil Aycam reports financial support was provided by Scientific and Technological Research Council of Turkey. If there are other authors, they declare that they have no known competing financial interests or personal relationships that could have appeared to influence the work reported in this paper.

Acknowledgement

The authors gratefully acknowledge the financial assistance of the Scientific and Technical Research Council (TUBITAK) of Türkiye, provided under Project: 122M562, and the Academic Writing Application and Research Centre at Gazi University for proofreading the article. This publication is part of the first author's doctoral thesis work at the Architecture Academic Programme of the Science Institute at Gazi University.

Data availability

Data will be made available on request.

References

[1] V.K. Dwivedi, P. Tiwari, S. Tiwari, Importance of Phase Change Material (PCM) in solar thermal applications: a review, in: 2016 International Conference on Emerging Trends in Electrical Electronics & Sustainable Energy Systems (ICETEESES), IEEE, 2016, pp. 42–45.

[2] B. Hojjati, S.H. Wade, US household energy consumption and intensity trends: a decomposition approach, Energy Policy 48 (2012) 304–314.

[3] R. Baetens, B.P. Jelle, A. Gustavsen, Phase change materials for building applications: a state-of-the-art review, Energ. Buildings 42 (9) (2010) 1361–1368.

[4] Y. Chihab, R. Bouferra, A. Bouchehma, Transient thermal behavior of clay walls integrated with phase change materials, J. Energy Storage 73 (2023) 109246, https://doi.org/10.1016/j.est.2023.109246.

[5] F. Kuznik, D. David, K. Johannes, J.J. Roux, A review on phase change materials integrated in building walls, Renew. Sust. Energ. Rev. 15 (1) (2011) 379–391.

[6] I. Rathore, R. Elangovan, S. Natarajan, Thermal performance profiling of phase change materials integrated building envelopes through simulation-data envelopment analysis approach, J. Energy Storage 153 (2026) 120947, https://doi.org/10.1016/j.est.2026.120947.

[7] U. Stritih, S. Medved, Use of phase change materials in the wall with TIM, Stroj Vestn-J Mech E 40 (3) (1994) 155–160.

[8] H. Manz, P.W. Egolf, P. Suter, A. Goetzberger, TIM–PCM external wall system for solar space heating and daylighting, Sol. Energy 61 (6) (1997) 369–379.

[9] N. Kienzl, Advanced Building Skins: Translucent Thermal Storage Elements, Massachusetts Institute of Technology, 1999 (Doctoral dissertation).

[10] J. Heim, Syn og lesing hos elever i grunnskolen, SINTEF, Trondheim, 2004.

[11] D. Heim, Whole year analysis of TIM-PCM solar thermal storage wall, Proc. SimBuild 1 (1) (2016).

[12] Y. Berthou, P.H. Biwole, P. Achard, H. Sallée, M. Tantot-Neirac, F. Jay, Full scale experimentation on a new translucent passive solar wall combining silica aerogels and phase change materials, Sol. Energy 115 (2015) 733–742.

[13] F. Souayfane, P.H. Biwole, F. Fardoun, Thermal behavior of a translucent superinsulated latent heat energy storage wall in summertime, Appl. Energy 217 (2018) 390–408.

[14] F. Souayfane, P.H. Biwole, F. Fardoun, P. Achard, Energy performance and economic analysis of a TIM-PCM wall under different climates, Energy 169 (2019) 1274–1291.

[15] C. Bekler, İ. Ayçam, M.Z. Yılmazoğlu, Analysis of thermal performance of an innovative thermal storage wall, J. Build. Eng. 103 (2025) 112058, https://doi.org/10.1016/j.jobe.2025.112058.

[16] M. Alama, J. Sanjayan, P.X.W. Zou, S. Ramakrishnan, J. Wilson, A comparative study on the effectiveness of passive and free cooling application methods of phase change materials for energy efficient retrofitting in residential buildings, Procedia Eng. 180 (2016) 993–1002.

[17] G. Evola, L. Marletta, F. Sicurella, A methodology for investigating the effectiveness of FDM wallboards for summer thermal comfort in buildings, Build. Environ. 59 (2013) 517–527.

[18] F. Fiorito, Trombe walls for lightweight buildings in temperate and hot climates exploring the use of phase change materials for performances improvement, Energy Procedia 30 (2012) 1110–1119.

[19] F. Guarino, S.L.M. Cellura, M. Mistretta, V. La Rocca, Phase change materials applications to optimize cooling performance of buildings in the Mediterranean area: a parametric analysis, Energy Procedia 78 (2015) 1708–1713.

[20] Y. Han, J.E. Taylor, Simulating the impact of phase change material embedded building envelopes on the inter-building effect in non-tropical cities, Procedia Eng. 118 (2015) 760–765.

[21] S. Li, N. Zhu, P. Hu, F. Lei, R. Deng, Numerical study on thermal performance of PCM Trombe Wall, Energy Procedia 158 (2019) 2441–2447.

[22] A.L. Pisello, Thermal-energy analysis of roof cool clay tiles for application in historic buildings and cities, Sustain. Cities Soc. 19 (2015) 271–280.

[23] S. Soudian, U. Berardi, Experimental investigation of latent thermal energy storage in highrise residential buildings in Toronto, Energy Procedia 132 (2017) 249–254.

[24] DesignBuilder, Welcome to DesignBuilder V7. https://designbuilder.co.uk/helpv7.0/index.htm. (Accessed 15 May 2025).

[25] M. Auzeby, S. Wei, C. Underwood, C. Chen, H. Ling, S. Pan, B. Ng, J. Tindall, R. Buswell, Using phase change materials to reduce overheating İssues in UK residential buildings, Energy Procedia 105 (2017) 4072–4077.

[26] S. Geitani, C. Chedid, C. Lahoud, J. Harmouche, S. Youssef, J. Kesserwani, Investigation of the optimal PCM wall location into buildings envelope under Mediteranean climate, in: 2025 7th International Conference on Renewable Energy for Developing Countries (REDEC), 2025, pp. 1–6.

[27] E. Köse, G. Manioğlu, Evaluation of the performance of phase change materials in relation to balanced distribution of heating energy cost in residential buildings, REHVA J. 55 (2) (2018) 52–57.

[28] A.F. Mohamed, M.M. Gomaa, A.A. Amir, A. Ragab, Energy, thermal, and economic benefits of aerogel glazing systems for educational buildings in hot arid climates, Sustainability 15 (8) (2022) 6332, https://doi.org/10.3390/su15086332.

[29] W.I.W.M. Nazi, Y. Wang, H. Chen, X. Zhang, A.P. Roskilly, Passive cooling using phase change material and insulation for high-rise office building in tropical climate, Energy Procedia 142 (2017) 2295–2302.

[30] D. Saylam Canım, S. Maçka Kalfa, Development of a new pumice block with phase change material as a building envelope component, J. Energy Storage 61 (2023) 106706, https://doi.org/10.1016/j.est.2023.106706.

[31] S.M. Sajjadian, J. Lewis, S. Sharples, The potential of phase change materials to reduce domestic cooling energy loads for current and future UK climates, Energ. Buildings 93 (2015) 83–89.

[32] Y. Zhang, Z. Zhu, Z. Peng, J. Luo, X. Sun, J. Li, F. Peng, The Trombe wall equipped with PCMs for the enhancement of the indoor thermal quality, Enerji ve Binalar 297 (2023) 113407, https://doi.org/10.1016/j.enbuild.2023.113407.

[33] Altensis, DesignBuilder software, URL: https://www.altensis.com/hizmetler/designbuilder-software/. (Accessed 15 May 2025).

[34] Meteotest, Meteonorm (Version 8.1.0), Meteotest AG, 2023. https://meteonorm.com (Software).

[35] E.H. Ahmad, Cost analysis and thickness optimization of thermal insulation materials used in residential buildings in Saudi Arabia, in: Proceedings of the 6th Saudi eng. Conference vol. 1, KFUPM, Dhahran, 2002, pp. 21–32.

[36] W. Kim, Y. Jeon, Y. Kim, Simulation-based optimization of an integrated daylighting and HVAC system using the design of experiments method, Appl. Energy 162 (2016) 666–674.

[37] J.F. Kreider, M. Anstett, Application of neural networking models to predict energy use, URL: https://www.aivc.org/sites/default/files/airbase_6524.pdf, 1993. (Accessed 11 August 2025).

[38] J. Mardaljevic, Daylight Simulation: Validation, Sky Models and Daylight Coefficients, De Montfort University, Leicester, 1999.

[39] J. Conraud-Bianchi, A Methodology for the Optimization of Building Energy, Thermal, and Visual Performance, Concordia University, Canada, Yüksek Lisans Tezi, 2008, p. 10s.

[40] J.A. Crabb, N. Murdoch, J.M. Penman, Building energy assessment by simplified dynamic simulation model, in: European Conference on Architecture, Munich, 1987.

[41] A. Hasan, Optimizing insulation thickness for buildings using life cycle cost, Appl. Energy 63 (2) (1999) 115–124.

[42] R. Ouarghi, M. Krarti, Building shape optimization using neural network and genetic algorithm approach, ASHRAE Trans. 112 (1) (2006).

[43] J. Han, M. Kamber, J. Pei, Data Mining: Concepts and Techniques, 3rd edition, Morgan Kaufmann Publishers, Waltham, 2012, pp. 120–124.

[44] X. Kong, S. Lu, Y. Li, J. Huang, S. Liu, Numerical study on the thermal performance of building wall and roof incorporating phase change material panel for passive cooling application, Energ. Buildings 81 (2014) 404–415.

[45] S.D. Zwanzig, Y. Lian, E.G. Brehob, Numerical simulation of phase change material composite wallboard in a multi-layered building envelope, Energy Convers. Manag. 69 (2013) 27–40.

[46] M. Biezma, J.S. Cristóbal, Investment criteria for the selection of cogeneration plants—a state of the art review, Appl. Therm. Eng. 26 (5–6) (2006) 583–588, https://doi.org/10.1016/j.applthermaleng.2005.07.006.

[47] BOTAŞ, BOTAŞ natural gas wholesale sales price tariff for August 2022, URL: https://www.botas.gov.tr/uploads/dosyaYoneticisi/949372-agustos_2022_tarifesi.pdf, 2022. (Accessed 31 October 2025).

[48] TÜİK, Turkish statistical institute: electricity and natural gas prices, first half: January–June 2022, URL: https://data.tuik.gov.tr/Bulten/Index?p=Elektrik-ve-Dogal-Gaz-Fiyatlari-I.-Donem:-Ocak-Haziran-2022-45567, 2022. (Accessed 31 October 2025).

[49] S.D. Mangan, G.K. Oral, Assessment of residential building performances for the different climate zones of Turkey in terms of life cycle energy and cost efficiency, Energ. Buildings 110 (2016) 362–376.

[50] F. Bilgin, M. Arıcı, Effect of phase change materials on time lag, DF and heat-saving, Acta Phys. Pol. A 132 (3) (2017) 1102–1105.

[51] D. Saylam Canım, Türkiye İklim Bölgelerinde Kullanima Uygun Yeni Nesil Hafif Bina Kabuğu Bileşeni Önerisi: Faz Değiştiren Malzemeli Pomza Blok, Karadeniz Technical University, Trabzon, Türkiye, 2022 (PhD Thesis).

[52] M. Katish, S. Allen, A. Squires, V. Ferrandiz-Mas, Thermal stability of organic Phase Change Materials (PCMs) by accelerated thermal cycling technique, Thermochim. Acta 737 (2024) 179771.

[53] V. Novik, Thermal and Optical Performance of Granular Aerogel Glazing After Accelerated Ageing, Toronto Metropolitan University. Canada, 2023 (MsC Thesis).

[54] B.L. Miller, D.E. Goldber, Genetic algorithms, tournament selection, and the effects of noise, Complex Systems 9 (3) (1995) 193–212.